American Mineralogist, Volume 70, pages 455–473, 1985

Towards a structural classification of minerals: The $^{VI}M^{IV}T_2\Phi_n$ minerals

F. C. HAWTHORNE

Department of Earth Sciences, University of Manitoba
Winnipeg, Manitoba, Canada R3T 2N2

Abstract

Cation bond-valence requirements are satisfied by their anion coordination polyhedra; anion bond-valence requirements are satisfied by the polymerization of these coordination polyhedra. When considered together with Pauling's second rule, this suggests that *structures may be ordered or classified according to the polymerization of those coordination polyhedra with higher bond-valences.* This is the basis of the approach to mineral classification proposed here, which focuses on the (two) types of coordination polyhedra of higher bond-valence. Minerals are divided into different sets according to their cation coordination numbers and cation stoichiometry, with a general group formula $M_xT_y\Phi_n$ (M and T are cations of different coordination number, Φ = unspecified ligand). Within a specific set, minerals are classified according to their basic heteropolyhedral cluster, or fundamental building block, and the way in which this cluster polymerizes to form a three-dimensional structure. Thus in each set are the following classes: (1) unconnected polyhedra; (2) finite clusters; (3) chains; (4) sheets; (5) frameworks.

The present work addresses the classification of minerals based on tetrahedra and octahedra, beginning with the $^{VI}M^{IV}T_2\Phi_n$ minerals. The 47 structure types of the 102 minerals of this set are analyzed in terms of their basic cluster and modes of polymerization, and organized into a structural hierarchy. The mode of polymerization of the fundamental building block is related to the Lewis basicity of the simple oxyanions $[(M\Phi_6) + 2(TO_4)]$ that constitute the cluster. The fundamental building block is repeated (often polymerized) by translational symmetry operators to form the *structure module*, a complex anionic polyhedral array whose excess charge is balanced by the presence of (usually) large low-valence cations. The Lewis basicity of the structure module may be related, via the valence matching principle, to the Lewis acidity of the extra-module cations. Using simple anion coordination numbers suggested by the valence sum rule, the coordination number of the extra-module cation can be calculated. This scheme predicts quite well the extra-module cation type and coordination number for the structures examined here. Mineral solubilities in water can also be rationalized using these arguments, and qualitative predictions of solubility are in good agreement with the limited amount of data available.

Introduction

A scientific classification is a distillation of our knowledge concerning the nature of the objects under consideration. This is reflected in the historical development of mineral classification from ancient times to the present day. Minerals were first classified according to their physical properties. From the initial work of Theophrastus and Pliny the Elder to the detailed work of Agricola and Biringucci, the improvements in mineral classification were based on more accurate observations of physical properties. At the beginning of the 19th century, contemporaneous with the extensive chemical studies of natural materials, came the chemical classifications of minerals. Initial work involved classification based on physical and chemical properties, but with the rapid advance of chemical knowledge, completely chemical classifications soon replaced these hybrid schemes. Berzelius was first to develop a system based on electronegative elements, in which classes of minerals are recognized by the common occurrence of anions and radicals, and this was greatly extended by Dana. Although there has been much revision in the ensuing period, the scheme of Dana is the only all-encompassing mineral classification and is still under active development today (Ferraiolo, 1982).

Early this century came the development of crystal-structure analysis. Characterization of mineral structures showed that the crystal structure (which encompasses the chemical composition) controls their physical and chemical properties, and probably also certain aspects of their paragenesis. Many mineralogists have suggested that crystal structure should be the basis of mineral classification. Except for a few *chemical* classes of minerals, this proposal has not been extensively developed; however, it is instructive to consider these classifications briefly. Bragg (1930) classified the silicates according to the ways in which the (SiO_4) tetrahedra polymerize; this has been developed fur-

0003–004X/85/0506–0455$02.00

ther by Zoltai (1960) and Liebau (1972, 1980). Pabst (1950) classified the aluminum hexafluorides according to the ways in which the (AlF_6) octahedra polymerize, and this has been developed further by Hawthorne (1984). The borates have been classified by Christ (1960) and Christ and Clark (1977) according to the ways in which the (BO_3) triangles and (BO_4) tetrahedra polymerize. Each of these classification schemes is based on the polymerizations of the principal anionic groups. However, such an approach to structure taxonomy is of little use in classes of minerals such as the phosphates or the sulphates, or even the nesosilicates, in which the principal anionic group does not self-polymerize. In addition, the interrelationships among structures involving different anionic groups are ignored. Moore (1980) has developed a successful classification for phosphates based on the polymerization of divalent and trivalent cation octahedra, a scheme which could also encompass some sulphates, arsenates, vanadates, etc. However, this scheme has the same disadvantage as the others, in that it focuses on just one part of the structure. This was recognized by Hawthorne (1979) and Moore (1980), both of whom suggested that a more adequate classification of phosphate minerals would be based on the polymerizations of octahedral–tetrahedral coordination polyhedra clusters.

All of these schemes have one thing in common; the basis on which the mineral class is defined is chemical rather than structural. The classes considered are silicates or borates, that is, chemical divisions rather than structural divisions. The resulting classifications are thus chemical-structural hybrids, in much the same way that the early chemical classifications were actually physical-chemical hybrids. A true structural classification should apply to all minerals, and should have as its basis structural rather than chemical considerations.

The development of a structural classification of minerals is part of the more general problem that is the development of a classification scheme for inorganic crystal structures. Considerable work has gone on in this area, particularly during the last ten or fifteen years. Much of this has concentrated on compounds of specific chemistry or bond type (e.g. Andersen, 1981; Parthe, 1981; Hulliger, 1981). With this restriction on composition, schemes of considerable sophistication have been developed; notable in this regard, and of considerable mineralogical interest is the work of Makovicky (1981) on bismuth-lead sulphosalts. More general approaches are afforded by the work of Loeb (1970), Lima-de-Faria and Figueiredo (1976), Andersen and Hyde (1982), O'Keefe and Hyde (1980) and Hellner (1984) among others. Much of the more general work centers on simple structures and minerals is not generally considered. An exception to this is the structural classification of minerals proposed by Lima-de-Faria (1983), which is based on the approach of Lima-de-Faria and Figueiredo (1976). This uses the idea of structural units, and categorizes structures according to the dimensionality of the unit polymerization; in this regard, there are some similarities with the methods introduced here. However, Lima-de-Faria (1983) emphasizes the layered aspect of structures, and the details of the schemes are interestingly dissimilar.

Preliminary considerations

Hawthorne (1983a) has proposed the following hypothesis: *structures may be ordered or classified according to the polymerization of those coordination polyhedra with higher bond-valences.* Such a hypothesis is suggested by Pauling's rules in the following manner. Cation bond-valence requirements are satisfied by the formation of anion coordination polyhedra around them; thus we can think of the structure as an array of complex anions, that polymerize in order to satisfy their anion bond-valence requirements. With regard to Pauling's second rule (Pauling, 1960), the most important polymerizations involve those coordination polyhedra with higher bond-valences, as these contribute most to the satisfaction of the anion bond-valence requirements. If the major imperative of a structure is the satisfaction of its cation and anion bond-valence requirements, the most important features of the structure are the type of cation coordination polyhedra and the way in which the coordination polyhedra of highest or higher bond-valences polymerize; this suggests the above hypothesis.

Hawthorne (1983a) has recently developed a graph theoretical method to derive all possible polyhedron clusters consonant with a given stoichiometry. This method is conceptually of interest when considering the question of structural classification of minerals, as it provides a link between the chemical formula of a mineral and its crystal structure, that is a link between the current chemical classification of minerals and the analogous structural arrangements. In principle, it is possible to derive all possible structures for a particular stoichiometry, but this approach is obviously not practical for such a general problem as mineral classification. In this case, it is more profitable to proceed in an inductive manner and analyze the structures observed for a specific stoichiometry in terms of polymerization of homo- or hetero-polyhedral clusters.

The fundamental polyhedral cluster or fundamental building block of a mineral structure could be defined as that array of polyhedra that is repeated by the operators of the lattice group to form the complete structure. Such a definition might be satisfactory if we were considering every polyhedron in the structure. However, this is not the case; we preferentially select polyhedra of high bond-valence and ignore the remaining low bond-valence polyhedra. Sometimes, the polyhedral cluster of interest has higher inherent symmetry (i.e., pseudo-symmetry) than the structure as a whole, and it is convenient to recognize this, as the fundamental cluster of high bond-valence polyhedra can be smaller than the asymmetric unit might originally suggest.

Minerals based on tetrahedral–octahedral clusters

The general methods adopted here are not restricted to any particular type or number of different coordination polyhedra. However, the present paper will concentrate on minerals in which the higher bond-valence polyhedra are tetrahedra and octahedra. All minerals involving tetrahedra and octahedra have been divided into different sets according to the stoichiometry of their octahedral and

tetrahedral components. They are given the general formula $M_xT_y\Phi_z$, where M = octahedrally coordinated cations, T = tetrahedrally coordinated cations, and Φ = unspecified ligand. This may also be written as $M_x(TO_4)_y\Phi_z$ if the tetrahedra are known to be unpolymerized. It should be emphasized that this general formula does not necessarily represent the complete formula of a mineral, but just the part involving the high bond-valence cation polyhedra.

It is sometimes not clear what is the most appropriate general formula for a mineral. For example, when both divalent and trivalent octahedrally coordinated cations are present on distinct sites, should they both be considered as M cations or should the divalent cations be omitted? Here I have generally omitted them on principle, unless they are disordered with the trivalent cations; however, this may not always be the best alternative, and a general answer may require *a posteriori* analysis. This is not overly important at the present stage, as the current results may require considerable reorganization once the initial classification process is complete.

Cluster polymerization

The possible modes of cluster polymerization can be divided into the following classes: (1) unconnected polyhedra; (2) isolated clusters; (3) chains; (4) sheets; (5) frameworks.

From a graphical viewpoint, (1) and (2) could be combined, but structurally it makes more sense to distinguish between them. Detailed classifications of each of these five types can be developed.

The $MT_2\Phi_n$ minerals

The present paper will consider the structural classification of the $MT_2\Phi_n$ minerals, part of the more general $M_xT_y\Phi_z$ minerals. The descriptions will stress the fundamental polyhedral cluster and the character of its polymerization, but the remainder of the structure will also be outlined as this shows systematic trends with variations in cluster chemistry for a fixed stoichiometry.

Isolated polyhedra

Minerals of this class are given in Table 1; the "cluster" has the general stoichiometry $MT_2\Phi_{14}$. The remaining bond-valence requirements of the anions are satisfied predominantly by H atoms, and thus the water molecule plays an important role in these structures. With the exception of the fleischerite group, all of these minerals contain $(M(H_2O)_6)$ octahedra. The progression from the amarillite group to the mendozite group to the alum group is characterized by an increasing degree of hydration. The bond-valence structure of the $(M(H_2O)_6)$ octahedra is the same throughout, and the additional water molecules are

Table 1. $MT_2\Phi_n$ minerals based on isolated $M\Phi_6$ octahedra and $T\Phi_4$ tetrahedra

Mineral	Formula	a(Å)	b(Å)	c(Å)	α(°)	β(°)	γ(°)	S.G.	Ref.
*Amarillite	$Na[Fe^{3+}(SO_4)_2(H_2O)_6]$	-	-	-		-		-	
Tamarugite	$Na[Al(SO_4)_2(H_2O)_6]$	7.353(2)	25.225(5)	6.097(2)		95.2(1)		$P2_1/a$	(1)
*Mendozite	$Na[Al(SO_4)_2(H_2O)_6]\cdot 5H_2O$	21.75(3)	9.11(10)	8.30(1)		92.47(8)		C2/c	(2)
Kalinite	$K[Al(SO_4)_2(H_2O)_6]\cdot 5H_2O$	-	-	-		-		-	
*Sodium alum	$Na[Al(SO_4)_2(H_2O)_6]\cdot 6H_2O$	12.214(1)						Pa3	(3)
Potassium alum	$K[Al(SO_4)_2(H_2O)_6]\cdot 6H_2O$	12.157(1)						-	
Tschermigite	$NH_4[Al(SO_4)_2(H_2O)_6]\cdot 6H_2O$	12.240(1)						-	
Apjohnite	$Mn[Al(SO_4)_2(H_2O)_6]_2\cdot 10H_2O$	6.198(2)	24.347(4)	21.266(4)		100.28(3)		$P2_1/c$	(4)
Bilinite	$Fe^{2+}[Fe^{3+}(SO_4)_2(H_2O)_6]_2\cdot 10H_2O$	-	-	-		-		-	
Dietrichite	$Zn[Al(SO_4)_2(H_2O)_6]_2\cdot 10H_2O$	-	-	-		-		-	
*Halotrichite	$Fe^{2+}[Al(SO_4)_2(H_2O)_6]_2\cdot 10H_2O$	6.181	24.297	20.519		100.99		$P2_1/c$	
Pickeringite	$Mg[Al(SO_4)_2(H_2O)_6]_2\cdot 10H_2O$	-	-	-		-		-	
Redingtonite	$Fe^{2+}[Cr(SO_4)_2(H_2O)_6]_2\cdot 10H_2O$	-	-	-		-		-	
Aubertite	$Cu^{2+}[Al(SO_4)_2(H_2O)_6]Cl\cdot 8H_2O$	6.282(3)	13.192(5)	6.260(3)	91.85(3)	94.70(3)	82.46(3)	$P\bar{1}$	(5)
Boussingaultite	$(NH_4)_2[Mg(SO_4)_2(H_2O)_6]$	6.211	12.597	9.324		107.22		$P2_1/c$	
Cyanochroite	$K_2[Cu(SO_4)_2(H_2O)_6]$	6.159(5)	12.131(7)	9.086(4)		104.45(5)		$P2_1/c$	(6)
Mohrite	$(NH_4)_2[Fe^{2+}(SO_4)_2(H_2O)_6]$	6.22	12.57	9.28		106.8		$P2_1/c$	
*Picromerite	$K_2[Mg(SO_4)_2(H_2O)_6]$	6.121(3)	12.25(3)	9.09(1)		104.2(1)		$P2_1/c$	(7)
Despujolsite	$Ca_3[Mn^{4+}(SO_4)_2(OH)_6]\cdot 3H_2O$	8.56(2)		10.76(4)					
*Fleischerite	$Pb_3[Ge(SO_4)_2(OH)_6]\cdot 3H_2O$	8.867(1)		10.875(1)				$P\bar{6}2c$	(8)
Schauertite	$Ca_3[Ge(SO_4)_2(OH)_6]\cdot 3H_2O$	8.529(1)		10.802(2)				$P\bar{6}2c$	

Ref.: (1) Robinson and Fang (1969). (2) Fang and Robinson (1972). (3) Cromer et al. (1967). (4) Menchetti and Sabelli (1976). (5) Ginderow and Cesbron (1979). (6) Carapezza and Riva di Sanseverino (1968). (7) Carapezza and Riva di Sanseverino (1970). (8) Otto (1975).

**indicates the name for this group of minerals, in Tables 1-8.*

Table 2. $MT_2\Phi_n$ minerals based on isolated $[(M(TO_4)_2\Phi_n)_m]$ clusters

Mineral	Formula	a(Å)	b(Å)	c(Å)	α(°)	β(°)	γ(°)	S.G.	Ref.
Anapaite	$Ca_2[Fe^{2+}(PO_4)_2(H_2O)_4]$	6.447(1)	6.816(1)	5.898(1)	101.64(3)	104.24(3)	70.76(4)	$P\bar{1}$	(1)
Bloedite	$Na_2[Mg(SO_4)_2(H_2O)_4]$	11.03	8.14	5.49		100.7		$P2_1/a$	(2,3)
Leonite	$K_2[Mg(SO_4)_2(H_2O)_4]$	12.03(3)	9.61(3)	9.98(4)		95.0(3)		C2/m	(4)
Schertelite	$(NH_4)_2[Mg(PO_3OH)_2(H_2O)_4]$	11.49(2)	23.66(6)	8.62(1)				Pbca	(5)
Roemerite	$Fe^{2+}[Fe^{3+}(SO_4)_2(H_2O)_4]_2\cdot 6H_2O$	6.463(8)	15.309(18)	6.341(8)	90.5(2)	101.1(2)	85.7(2)	$P\bar{1}$	(6)
Metavoltine	$K_2Na_6Fe^{2+}[Fe_3^{3+}(SO_4)_6O(H_2O)_3]_2\cdot 12H_2O$	9.575(5)		18.17(1)				P3	(7)

Ref.: (1). Catti et al. (1979). (2). Rumanova and Malitskaya (1960). (3). Bukin and Nozik (1975). (4). Srikanta et al. (1968). (5). Khan and Baur (1972). (6). Fanfani et al. (1970a). (7). Giacovazzo et al. (1976).

added to the coordination polyhedra of the alkali cation to replace the oxygen of the (SO_4) tetrahedra, which no longer coordinate the alkali cation. These additional water molecules form hydrogen bonds to the oxygens of the (SO_4) tetrahedra, further linking the structures together. The alum structure actually forms the end member of this series at the present time. Increased states of hydration could occur, but would entail either an increase in the alkali cation coordination number, or the addition of water held in the structure solely by hydrogen bonding. This type of water occurs in the minerals of the halotrichite group, which are characterized by $(M^{3+}(H_2O)_6)$ octahedra with electroneutrality being maintained by the presence of $(M^{2+}O(H_2O)_5)$ octahedra that are not considered to be an M-type cation here. Thus there are five H_2O molecules in the formula unit of these minerals that are not directly bonded to a cation; nonetheless, these water molecules are an essential part of the structure (i.e. non-zeolitic), being held in place by hydrogen bonding. *A priori*, it is not clear whether or not the minerals of the halotrichite group should be considered as $MT_2\Phi_n$ or as $M_3T_4\Phi_n$ minerals; however, as shown later, they can be satisfactorily interpreted as $MT_2\Phi_n$ minerals. The same situation exists for aubertite, consisting of discrete (SO_4) tetrahedra and $(Al(H_2O)_6)$ polyhedra, together with a $(Cu(H_2O)_6)$ octahedron, Cl^-, and two H_2O molecules that are only involved in hydrogen bonding. Again, it will be shown that the observed bond connectivity is consistent with its interpretation as an $MT_2\Phi_n$ structure.

The minerals of the picromerite group are characterized by a divalent M cation, forming an $(M^{2+}(H_2O)_6)$ octahedron that hydrogen bonds to the oxygens of the (SO_4) tetrahedra. The alkali cations satisfying electroneutrality are K and NH_4, cations, and it is perhaps significant that there are no Na members in this group. The minerals of the fleischerite group are different in that they contain an $(M(OH)_6)$ octahedron; this results in very weak hydrogen bonding from this octahedron to the rest of the structure. The water of hydration has the same role in this structure as in the mendozite and alum groups, augmenting the coordination polyhedron of the large lower-valence cations.

Finite clusters

Minerals whose structures are based on finite clusters of tetrahedra and octahedra are given in Table 2. There are three different kinds of clusters, and these are illustrated in Figure 1. Anapaite, bloedite, leonite and schertelite are based on the simple $[M(T\Phi_4)_2\Phi_4]$ cluster with the tetrahedra arranged in a *trans* configuration relative to the octahedron (Fig. 1b); this cluster is compatible with a center of symmetry at the octahedral cation, and in the first three minerals the cluster has this point symmetry. In these four minerals, the M cation is divalent and all four of the "unspecified ligands" (Φ_4) of the cluster are (H_2O). Roemerite is also based on a simple $M(T\Phi_4)_2\Phi_4$ cluster, but in this structure the tetrahedra are arranged in a *cis* configuration (Fig. 1a) relative to the octahedron; this cluster is not compatible with a center of symmetry. The formula of roemerite (Table 2) has been written to emphasize the presence of this $[M(TO_4)_2\Phi_4]$ cluster. The charge-balancing Fe^{2+} is coordinated by six water molecules, and thus the roemerite structure consists of an $(Fe^{2+}(H_2O)_6)$ octahedron and two $[Fe^{3+}(SO_4)_2(H_2O)_4]$ clusters linked together solely by hydrogen bonding. The structure of metavoltine is based on a complex but elegant cluster of composition $[M_3(TO_4)_6O_4]$ (Fig. 1c) that is also found in a series of synthetic compounds investigated by Scordari (1980, 1981a). As in all of these "isolated cluster" structures, hydrogen bonding plays an important part in the inter-cluster linkage.

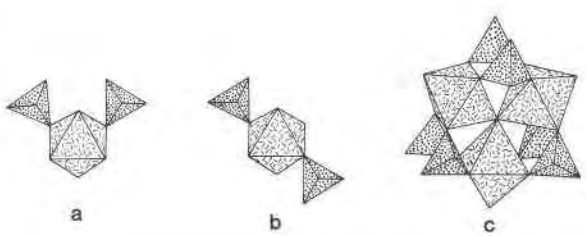

Fig. 1. Finite $[M(TO_4)_2\Phi_n]$ clusters found in minerals: (a) *cis* $[M(TO_4)_2\Phi_4]$; (b) *trans* $[M(TO_4)_2\Phi_4]$; (c) $[M_3(TO_4)_6\Phi_4]$.

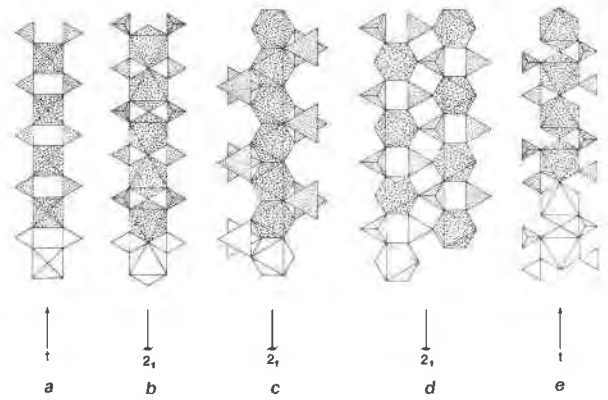

Fig. 2. Infinite $[M(TO_4)_2\Phi_n]$ and $[M_2(TO_4)_4\Phi_n]$ chains found in minerals: (a) $[M(TO_4)_2\Phi_2]$ = kröhnkite-type; (b) $[M(TO_4)_2\Phi]$ = tancoite-type; (c) $[M(TO_4)_2\Phi]$ = brackebuschite-type; (d) $[M(TO_4)_2\Phi]$ = ransomite-type; (e) $[M_2(TO_4)_4\Phi_5]$ = botryogen-type. The fundamental $[M(TO_4)_2\Phi_4]$ and $[M_2(TO_4)_4\Phi_n]$ clusters are shown unshaded, and the repetition operator is shown.

Infinite chains

A large number of infinite chains of the forms $[M(TO_4)_2\Phi_n]$ and $[M_2(TO_4)_4\Phi_n]$ can be built up from simple $[M(TO_4)_2\Phi_n]$ clusters. Only a few types have thus far been found in minerals (schematically illustrated in Fig. 3), although many more types are found in synthetic inorganic compounds. The simplest (least connected) type of chain is the $[M(TO_4)_2\Phi_2]$ chain (Fig. 2a) that is the basis of the minerals of the kröhnkite group, the talmessite group and the fairfieldite group (Table 3). In each group, the $[M(TO_4)_2\Phi_2]$ chain is parallel to the **c**-axis with a repeat distance of ~5.55Å. The three structure types (Fig. 3) differ principally in the hydrogen bonding schemes developed in each.

Next is the $[M(TO_4)_2\Phi]$ chain (Fig. 2b) that is the basis of the minerals listed in Table 4. The repeat distance of the chain is ~7.20Å or some multiple of this value, and is normally evident in the cell dimensions (Table 4). The complexity of these structures is much greater than that exhibited by the minerals of Table 3. Perhaps the simplest structure is tancoite (Fig. 4a), in which the $[M(TO_4)_2\Phi]$ chains are in a square array (Fig. 4b), cross-linked by alkali cations and hydrogen bonds. Scordari (1981b) has proposed that the sideronatrite structure contains this same $[M(TO_4)_2\Phi]$ chain. The general stoichiometry and unit cell dimensions suggest (Hawthorne, 1983b) that the sideronatrite structure may be a supercell derivative of the *Acmm* tancoite substructure. Similarly, metasideronatrite (I) may also have a tancoite-derivative structure. The structures of the minerals of the jahnsite and the segelerite groups consist of slabs of tancoite-like structure, intercalated with slabs of $(M^{2+}O_2(H_2O)_4)$ octahedra, as shown in Figure 5. Moore and Araki (1977) refer to jahnsite and segelerite as combinatorial polymorphs, and they give an elegant discussion of the relationships between both these two observed structures and other feasible structural arrangements. The basic structural difference between these two minerals depends on the nature of $(M^{2+}O_2(H_2O)_4)$ linking octahedra; in the segelerite structure (Fig. 5), the linkage between the tancoite-like slabs is always *trans*, whereas in the jahnsite structure, the linkage is both *trans* (through the Mg(1) octahedron) and *cis* (through the Mg(2) octahedron).

The guildite structure is based on $[Fe(SO_4)_2(OH)]$ chains that are bound together by $(CuO_2(H_2O)_4)$ octahedra (Fig. 6). The structure can be considered as a collapsed version of the segelerite structure with no interchain Ca cations present; the $(CuO_2(H_2O)_4)$ octahedra play the same interchain bridging role that the $(MgO_2(H_2O)_4)$ octahedra do in segelerite. The yftisite structure is based on $[Ti(SiO_4)_2O]$ chains (Fig. 6), also of the tancoite type, bound together by [7]- and [8]-coordinated Y^{3+} cations.

The $[M(TO_4)_2\Phi]$ chain (Fig. 2c) is the basis of the structures of the brackebuschite minerals, encompassing the brackebuschite, fornacite and vauquelinite groups (Table

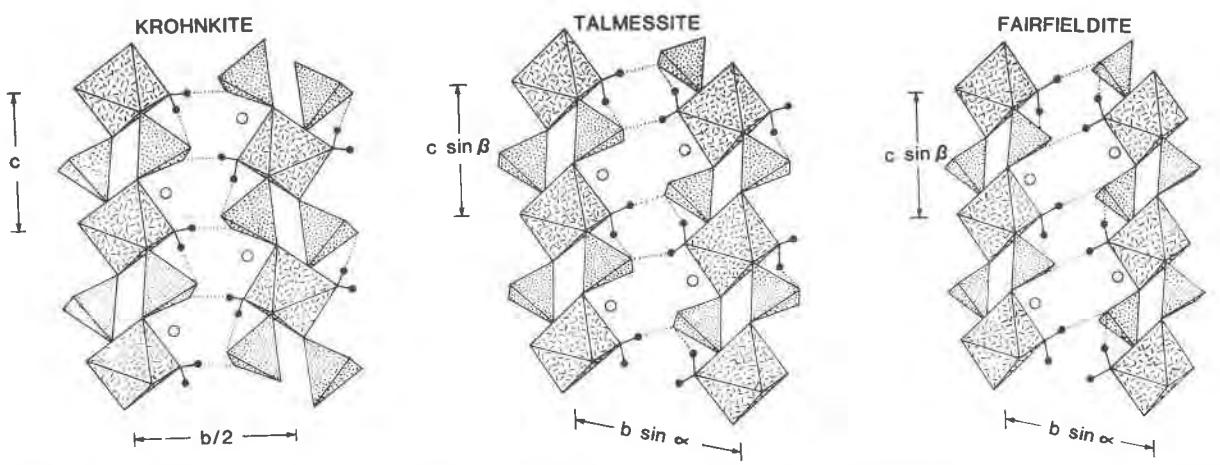

Fig. 3. The structures of the kröhnkite, talmessite and fairfieldite groups, all based on the $[M(TO_4)_2\Phi_2]$ type chain shown in Figure 2a. Different hydrogen-bonding arrangements between adjacent chains characterize each structure.

Table 3. $MT_2\Phi_n$ minerals based on the infinite $[M(TO_4)_2\Phi_2]$ chain shown in Fig. 3a

Mineral	Formula	a(Å)	b(Å)	c(Å)	α(°)	β(°)	γ(°)	S.G.	Ref.
Brandtite	$Ca_2[Mn(AsO_4)_2(H_2O)_2]$	5.899(2)	12.968(4)	5.684(1)		108.05(2)		P2,/c	(1)
*Kröhnkite	$Na_2[Cu(SO_4)_2(H_2O)_2]$	5.807(1)	12.656(2)	5.517(1)		108.32(1)		P2,/c	(2)
Roselite	$Ca_2[(Co,Mg)(AsO_4)_2(H_2O)_2]$	5.801(1)	12.898(3)	5.617(1)		107.42(2)		P2,/c	(1)
Cassidyite	$Ca_2[Ni(PO_4)_2(H_2O)_2]$	5.713(13)	6.730(15)	5.430(11)	96.7(2)	107.3(3)	104.7(2)	P$\bar{1}$	(3)
Collinsite	$Ca_2[Mg(PO_4)_2(H_2O)_2]$	5.734(1)	6.780(1)	5.441(1)	97.29(1)	108.56(1)	107.28(1)	P$\bar{1}$	(3,4)
Gaitite	$Ca_2[Zn(AsO_4)_2(H_2O)_2]$	5.915(5)	6.981(6)	5.572(6)	96.70(9)	108.76(6)	107.40(6)	P$\bar{1}$	(5)
Roselite-beta	$Ca_2[Co(AsO_4)_2(H_2O)_2]$	5.884(6)	6.963(8)	5.581(9)	97.72(8)	109.24(9)	107.5(1)	P$\bar{1}$	(4)
*Talmessite	$Ca_2[Mg(AsO_4)_2(H_2O)_2]$	5.884(4)	6.995(4)	5.564(4)	97.69(9)	109.7(1)	107.9(1)	P$\bar{1}$	(4)
*Fairfieldite	$Ca_2[Mn(PO_4)_2(H_2O)_2]$	5.79(1)	6.57(1)	5.51(1)	102.3(3)	108.7(3)	90.3(3)	P$\bar{1}$	(6)
Messelite	$Ca_2[Fe^{2+}(PO_4)_2(H_2O)_2]$	5.95(2)	6.52(2)	5.45(2)	102.3(4)	107.5(4)	90.8(2)	P$\bar{1}$	(4)

Ref.: (1) Hawthorne and Ferguson (1977). (2) Hawthorne and Ferguson (1975). (3) Brotherton et al. (1974). (4) Catti et al. (1977). (5) Sturman and Dunn (1980), cell re-fined in reduced cell orientation. (6) Fanfani et al. (1976b).

5). The chain runs parallel to the **b**-axis in these minerals, and has a characteristic repeat distance of ~5.29Å. The atomic arrangements are very similar in all three structure types, the $[M(TO_4)_2\Phi]$ chains being cross-linked by high-coordination ([9]-, [10]- and [11]-coordinate) divalent and trivalent cations (Fig. 7, Table 5). Minor changes in the coordination (bond-valence) requirements of the large cations lead to the differences in symmetry among the three structure types; this is discussed in detail by Fanfani and Zanazzi (1968, 1969) and Shen and Moore (1982).

The crystal structures of ransomite and krausite (Table 6) are based on a slightly more complex type of $[M(TO_4)_2\Phi_n]$ chain. These structures are shown in Figure 8, in which it can be seen that the chains are graphically identical to each other, and have the general stoichiometry $[M(TO_4)_2\Phi]$. The chain can be constructed from a *cis* $M(TO_4)_2$ cluster that is repeated by a 2_1 screw operator as shown in Figure 2d. The original cluster links to clusters that are equivalent by virtue of the 2_1 operation *and* the t (translation) operation parallel to the length of the chain; thus the chain is broader than the chains discussed previously.

Although not apparent from the chemical formula, the structure of botryogen (Table 6) is based on an

Table 4. $MT_2\Phi_n$ minerals based on the infinite $[M(TO_4)_2\Phi]$ chain shown in Fig. 3b

Mineral	Formula	a(Å)	b(Å)	c(Å)	β(°)	S.G.	Reference
Tancoite	$Na_2Li[Al(PO_4)_2(OH)]H$	6.948(2)	14.089(4)	14.065(3)		Pbcb	(1)
†Sideronatrite	$Na_2[Fe^{3+}(SO_4)_2(OH)]\cdot 3H_2O$	7.29(1)	20.56(2)	7.17(2)		Pnn2	(2)
*Jahnsite	$CaMnMg_2[Fe^{3+}(PO_4)_2(OH)]_2\cdot 8H_2O$	14.94(2)	7.14(1)	9.93(1)	110.16(8)	P2/a	(3)
Whiteite	$CaFe^{2+}Mg_2[Al(PO_4)_2(OH)]_2\cdot 8H_2O$	14.90(4)	6.98(2)	10.13(2)	113.11(9)	P2/a	(4)
Lun'okite	$Mn_2(Mg,Fe^{2+},Mn)_2[Al(PO_4)_2(OH)]_2\cdot 8H_2O$	14.95	18.71	6.96		Pbca	-
Overite	$Ca_2Mg_2[Al(PO_4)_2(OH)]_2\cdot 8H_2O$	14.72(1)	18.75(2)	7.107(4)		Pbca	(5)
*Segelerite	$Ca_2Mg_2[Fe^{3+}(PO_4)_2(OH)]_2\cdot 8H_2O$	14.826(5)	18.751(4)	7.307(1)		Pbca	(5)
Wilhelmvierlingite	$Ca_2Mn_2[Fe^{3+}(PO_4)_2(OH)]_2\cdot 8H_2O$	14.80(5)	18.50(5)	7.31(2)		Pbca	-
Guildite	$Cu^{2+}[Fe^{3+}(SO_4)_2(OH)]\cdot 4H_2O$	9.786(2)	7.134(1)	7.263(1)	105.38(1)	P2,/m	(6)
Yftisite	$Y_4[Ti(SiO_4)_2O](F,OH)_6$	14.949(4)	10.626(2)	7.043(2)		Cmcm	(7)

References: (1) Hawthorne (1983b). (2) Scordari (1981b). (3) Moore and Araki (1974). (4) Moore and Ito (1978). (5) Moore and Araki (1977). (6) Wan et al. (1978). (7) Balko and Bakakin (1975).

†*structure not definitively established.*

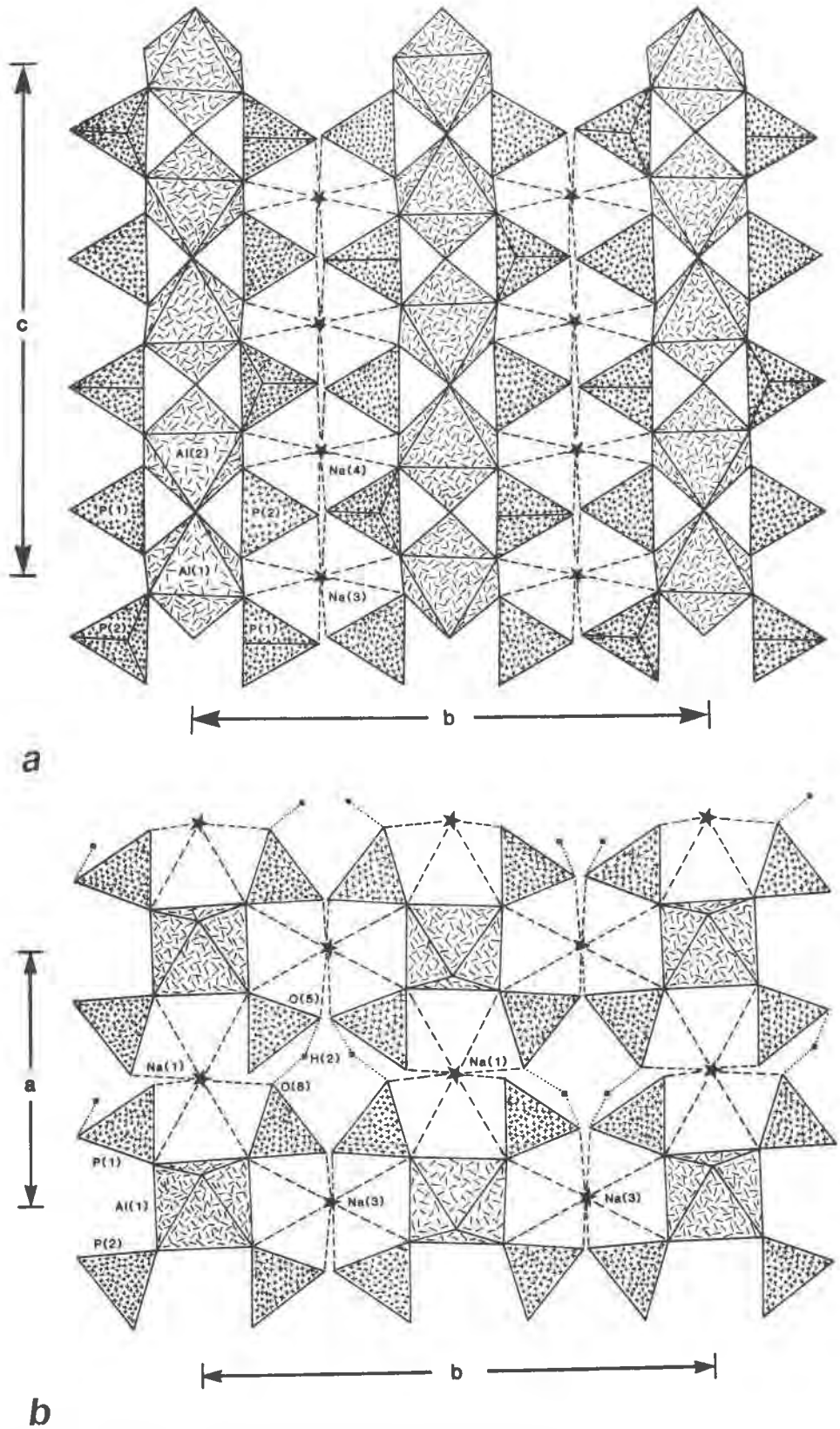

Fig. 4. The structure of tancoite, showing the constitution of the $[M(TO_4)_2\Phi]$ chains (Fig. 2b), and their relative arrangement and binding by interstitial sodium cations and hydrogen bonding; from Hawthorne (1983c).

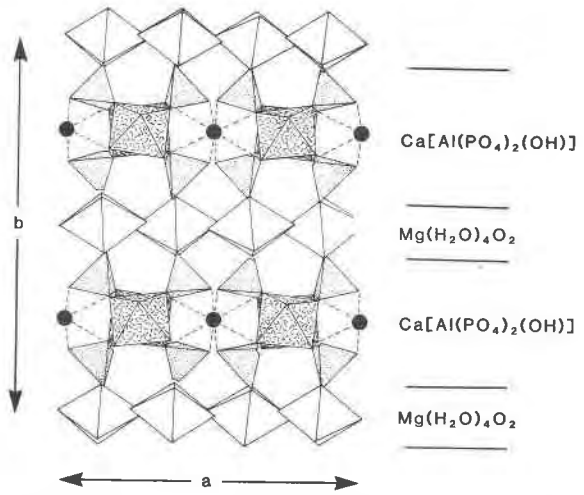

Fig. 5. The structure of segelerite, after Moore and Araki (1977). The $[M(TO_4)_2\Phi]$ tancoite-type chains (shaded) run parallel to **c** and are cross-linked into slabs on (010) by Ca cations; the slabs are linked together by layers of $(Mg(H_2O)_4O_2)$ octahedra in which the oxygens are arranged *cis* to the central Mg cation.

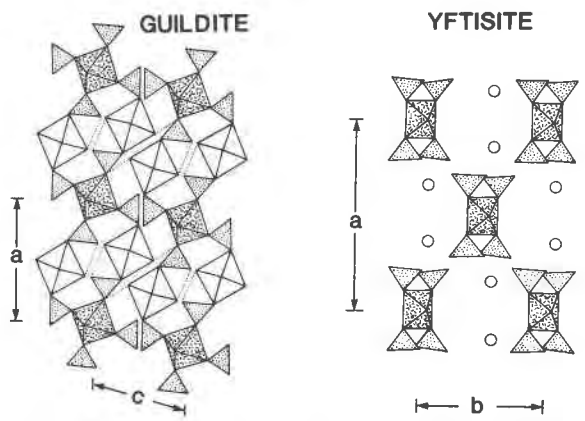

Fig. 6. The structures of guildite (left) and yftisite (right), both based on the $[M(TO_4)_2\Phi]$ tancoite-type chain, seen in each structure in cross-section; interchain bonding is by $(Cu(H_2O)_4O_2)$ octahedra in guildite and [7]- and [8]-coordinated Y^{3+} in yftisite.

$[M_2(TO_4)_4\Phi_5]$ cluster that is repeated by simple translation to give an infinite chain of composition $[M_2(TO_4)_4\Phi_4]$ having the structure shown in Figure 2e. Alternate octahedra along the chain are graphically distinct, and thus the heteropolyhedral cluster that forms the fundamental building block contains two distinct octahedra, not one as found in the simpler chains described earlier. The chains are linked to divalent cation octahedra of the form $(X(H_2O)_5O)$ through a network of hydrogen bonds.

Infinite sheets

The minerals of this category (Table 7) are based on three distinct types of infinite sheets. The simplest sheet is the $[M(TO_4)_2\Phi_2]$ sheet (Fig. 9a) that is the basis of the structure of rhomboclase. The fundamental building block is a *cis* $[M(TO_4)_2\Phi_4]$ cluster that is repeated in two dimensions to form a rather open sheet involving M–T corner-sharing only. In rhomboclase, these sheets are joined by a complex of hydrogen bonds involving interlayer H_5O_2 groups.

The $[M(TO_4)_2\Phi_2]$ sheet (Fig. 9b) is the basis of the olmsteadite structure and has the composition $[Nb(PO_4)_2O_2]$. The basic *cis* $[M(TO_4)_2\Phi_4]$ cluster is repeated to form a rather open sheet involving octahedral-tetrahedral corner-linking only; these linkages through the $M\Phi_6$ octahedron are *cis* ‖Y and *trans* ‖Z. In the olmsteadite structure, the sheets are joined by Fe^{2+}, K and by hydrogen bonds. Note that the first and second sheets in Figure 9a, b are graphically equivalent, and are in fact geometrical isomers.

Table 5. $MT_2\Phi_n$ minerals based on the infinite $[M(TO_4)_2\Phi]$ chain shown in Fig. 3c

Mineral	Formula	a(Å)	b(Å)	c(Å)	β(°)	S.G.	Reference
Arsenbrackebuschite	$Pb_2[Fe^{2+}(AsO_4)_2(H_2O)]$	7.763(1)	6.046(1)	9.022(1)	112.5(1)	$P2_1/m$	(1)
Arsentsumebite	$Pb_2[Cu(SO_4)(AsO_4)(OH)]$	7.84	5.92	8.85	112.6	$P2_1/m$	-
*Brackebuschite	$Pb_2[Mn(VO_4)_2(H_2O)]$	7.68	6.18	8.88	111.8	$P2_1/m$	(2)
Gamagarite	$Ba_2[(Fe^{3+},Mn)(VO_4)_2(OH,H_2O)]$	7.88(1)	6.17(1)	9.15(1)	112.7(1)	$P2_1/m$	-
Goedkenite	$Sr_2[Al(PO_4)_2(OH)]$	7.26(2)	5.74(2)	8.45(2)	113.7(1)	$P2_1/m$	(3)
Tsumebite	$Pb_2[Cu(PO_4)(SO_4)(OH)]$	7.85	5.80	8.70	111.5	$P2_1/m$	(4)
*Fornacite	$Pb_2[Cu(AsO_4)(CrO_4)(OH)]$	8.101(7)	5.892(11)	17.547(9)	110.00(3)	$P2_1/c$	(5)
Molybdofornacite	$Pb_2[Cu(AsO_4)(MoO_4)(OH)]$	8.100(5)	5.946(3)	17.65(1)	109.17(5)	$P2_1/c$	-
Tornebohmite	$(RE)_2[Al(SiO_4)_2(OH)]$	7.383(3)	5.673(3)	16.937(6)	112.04(2)	$P2_1/c$	(6)
Vauquelinite	$Pb_2[Cu(PO_4)(CrO_4)(OH)]$	13.754(5)	5.806(6)	9.563(3)	94.56(3)	$P2_1/n$	(7)

References: *(1) Hofmeister and Tillmanns (1978). (2) Donaldson and Barnes (1955). (3) Moore et al. (1975). (4) Nichols (1966). (5) Cocco et al. (1967). (6) Shen and Moore (1982). (7) Fanfani and Zanazzi (1968).*

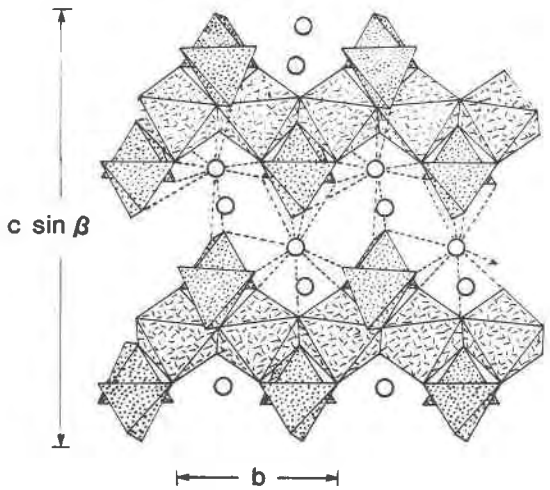

Fig. 7. The structure of törnebohmite, based on the $[M(TO_4)_2\Phi]$ brackebuschite-type chain shown in Figure 2c; after Shen and Moore (1982). The chains run parallel to **b** and are cross-linked by RE cations in törnebohmite, and large alkaline-earth cations in the brackebuschite- and vauquelinite-group minerals.

The more complex $[M(TO_4)_2]$ sheet of Figure 9c is the basis of the merwinite, brianite and yavapaiite structures, two of which are illustrated in Figure 10. The sheet can be derived from a *cis* $[M(TO_4)_2\Phi_4]$ cluster that is repeated by translations, such that the polymerization involves M–T corner-sharing only. In yavapaiite (Fig. 10), the sheet is graphically identical but symmetrically distinct from the ideal sheet of Figure 9c. In merwinite, the $[Mg(SiO_4)_2]$ sheets are bonded together by [8]- and [9]-coordinate Ca; in brianite, the $[Mg(PO_4)_2]$ sheets are similarly bonded together by [8]- and [9]-coordinate Na and Ca. In yavapaiite, the sheets are bonded together by [10]-coordinate K. The observed cell-dimensions are related to those of the ideal sheet (merwinite, obs. (calc.), $b = 5.29(5.57)$, $c = 9.33(9.56)$; brianite, obs. (calc.), $b = 5.23(5.45)$, $c = 9.13(9.44)$; yavapaiite, obs. (calc.), $a = 8.15(9.04)$, $b = 5.15(5.22)$Å), but the departures away from the ideal values are considerable.

The structure of bafertisite is based on an elegantly simple $[M(T_2O_7)\Phi_2]$ sheet (Fig. 9d); this is most easily constructed from a *cis* $[M(TO_4)_2\Phi_4]$ cluster linked in one direction by M–T corner-sharing and is the other direction by T–T corner linkage. In bafertisite, these sheets of composition $[Ti(Si_2O_7)O_2]$ are linked alternately by layers of [6]-coordinate Fe^{2+} and [10]-coordinate Ba.

The next type of sheet to be considered is the $[M(T_2O_5)\Phi]$ sheet (Fig. 9e) that involves M–M edge-sharing, M–T corner-sharing and T–T corner-sharing, and is formed from the *cis* $[MTO_4)_2\Phi_4]$ cluster. This sandwich-like sheet is the basis of several important structures (Table 7). In pyrophyllite, the sheets are held together solely by hydrogen bonding, whereas in the dioctahedral micas, the clay minerals of the illite group, and the dioctahedral brittle micas, the sheets are held together by alkali and alkali-earth cations. On the basis of the hypothesis proposed earlier, several minerals traditionally classed as trioctahedral micas are included here; these are zinnwaldite, ephesite and taeniolite. The Li–O bond-valence is ~0.17 v.u., whereas the Al–O bond-valence is ~0.50 v.u.; on this basis, $Li\Phi_6$ octahedra are not included in the basic unit which consequently is that shown in Figure 9e.

The last mineral in this class is goldichite; part of the structure is shown in Figure 11. It is based on an $[M_2(TO_4)_4\Phi_6]$ cluster, heavily shaded in Figure 11, that is repeated parallel to a, to form a very thick corrugated sheet parallel to (100). Individual clusters are joined by one M–T corner-sharing linkage, and the rather open sheets that are formed are bonded together by [9]-coordinate K and a network of hydrogen bonds.

Framework structures

The minerals of this class are listed in Table 8, arranged in order of increasing complexity of cluster polymerization. Perhaps the simplest of the framework structures is keldyshite (Fig. 12). The basic *cis* $[M(TO_4)_2\Phi_4]$ cluster is repeated with M–T corner-sharing in two directions to form a sheet ∥(100). This sheet is repeated by simple translation ∥**a** such that adjacent sheets are linked by sharing tetrahedral corners to form pyro-groups in the three-dimensional structure. The complete inter-cluster linkage is thus M–T and T–T corner-sharing.

The structure of nenadkevichite (Fig. 13) is also based on a simple *cis* $[M(TO_4)_2\Phi_4]$ cluster. This cluster is repeated

Table 6. $MT_2\Phi_n$ minerals based on the infinite $[M(TO_4)_2\Phi]$ and $[M_2(TO_4)_4\Phi_4]$ chains shown in Fig. 3d and 3e

Mineral	Formula	a(Å)	b(Å)	c(Å)	β(°)	S.G.	Ref.
Ransomite	$Cu^{2+}[Fe^{3+}(SO_4)_2(H_2O)]_2\cdot 4H_2O$	4.811(2)	16.217(4)	10.403(2)	93.02(3)	P2₁/c	(1)
Krausite	$K[Fe^{3+}(SO_4)_2(H_2O)]$	7.908(10)	5.152(5)	8.988(10)	102.75(8)	P2₁/m	(2)
*Botryogen	$Mg_2[Fe_2^{3+}(SO_4)_4(OH)_2(H_2O)_2]\cdot 10H_2O$	10.47	17.83	7.11	100.3	P2₁/n	
Zincbotryogen	$Zn_2[Fe_2^{3+}(SO_4)_4(OH)_2(H_2O)_2]\cdot 10H_2O$	10.526(4)	17.872(7)	7.136(4)	100.13(4)	P2₁/n	(3)

Ref.: (1) Wood (1970). (2) Graeber et al. (1965). (3) Susse (1968).

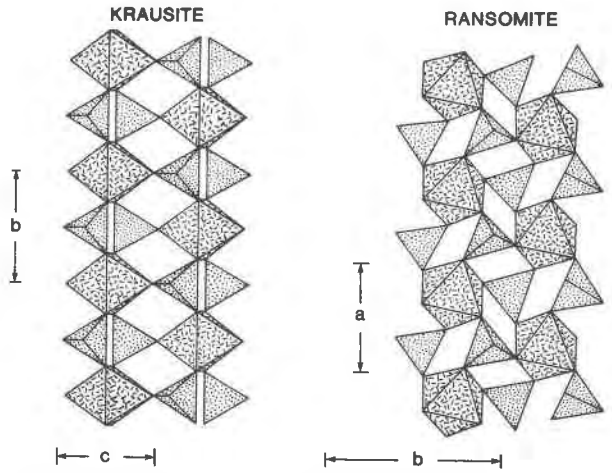

Fig. 8. The structures of krausite (left) and ransomite (right), based on the $[M(TO_4)_2\Phi]$ chain shown in Figure 2d.

by M–M and M–T corner-sharing linkages ‖**c** to form a (tancoite-like) chain of the kind shown in Figure 2b. This chain is repeated by T–T corner-sharing linkage ‖**a** and **b** (Fig. 13a) to form the basic framework (Fig. 13b); note the four-membered tetrahedral rings. The alkali cations provide additional linkage within the framework, together with a small amount of hydrogen bonding. Labuntsovite, the Ti analogue of nenadkevichite, is monoclinic, but the structure is virtually the same as that of nenadkevichite.

The structure of batisite and shcherbakovite is shown in Figure 14. Again the basic element is the *cis* $[M(TO_4)_2\Phi_4]$ cluster; this is repeated to form the sheet shown in Figure 14a, with M–T corner-linkage ‖**a** and T–T corner-linkage ‖**b**. This sheet is repeated ‖**c** with M–M and T–T corner-sharing linkages to form the framework structure of Figure 14b. The large alkali and alkaline-earth cations occupy the large voids apparent in Figure 14.

Next is a more familiar structure, that of the alkali and calcic pyroxenes. The basic *cis* $[M(TO_4)_2\Phi_4]$ cluster (Fig. 15) is repeated ‖**c**, such that there is edge-sharing between octahedra, corner-sharing between tetrahedra, and corner-sharing between octahedra and tetrahedra; this forms the familiar chain-like fragment of the pyroxene structure. This is repeated ‖**a** and **b**, with corner-sharing between octahedra and tetrahedra, to give the resulting pyroxene framework.

The last three structures, låvenite, wöhlerite and rosenbuschite, show an interesting progression in the complexity of the fundamental cluster, Låvenite is formed from the basic *cis* $[M(TO_4)_2\Phi_4]$ cluster that is repeated in two dimensions with corner-sharing between octahedra and tetrahedra; this sheet is then repeated with corner-sharing between tetrahedra of adjacent sheets. Wöhlerite is formed from a more complex $[M_2(TO_4)_4\Phi_6]$ cluster, in which the two octahedra are graphically distinct; this cluster is re-

Table 7. $MT_2\Phi_n$ minerals based on infinite sheets

Minerals	Formula	a(Å)	b(Å)	c(Å)	β(°)	S.G.	Ref.
Rhomboclase	$H_5O_2[Fe^{3+}(SO_4)_2(H_2O)_2]$	9.724(4)	18.333(9)	5.421(4)		Pnma	(1)
Olmsteadite	$KFe^{2+}_2[Nb(PO_4)_2O_2]\cdot 2H_2O$	7.512(1)	10.000(3)	6.492(2)		Pb2,m	(2)
Brianite	$Na_2Ca[Mg(PO_4)_2]$	13.36(5)	5.23(2)	9.13(3)	91.2(2)	P2,/a	(3)
*Merwinite	$Ca_3[Mg(SiO_4)_2]$	13.25(2)	5.293(9)	9.33(2)	91.9(2)	P2,/a	(4)
Yavapaiite	$K[Fe^{3+}(SO_4)_2]$	8.152(5)	5.153(4)	7.877(5)	94.90(7)	C2/m	(5)
Bafertisite	$BaFe^{2+}[TiSi_2O_7O_2]$	10.60	13.64	12.47	119.5	C2/m	(6)
Pyrophyllite	$[AlSi_2O_5(OH)]_2$	5.161(2)	8.958(2)	9.351(2)	100.37(2)	$C\bar{1}^+$	(7)
Dioctahedral Micas	$(M^+,M^{2+})[(M^{3+},M^{2+})(Si,Al)_2O_5(OH)]_2$	~5.2	~9.0	~10.0	~100.0	C2/m	(8)
Ephesite	$NaLi[Al(Si,Al)_2O_5(OH)]_2$	5.27	9.13	10.25	100.0	C2/m	
Taeniolite	$KLi[MgSi_2O_5(OH)]_2$	5.231(1)	9.065(2)	10.140(1)	99.86(2)	C2/m	(9)
Dioctahedral Smectites	$(M^+,H_2O)[(M^{3+},M^{2+})(Si,Al)_2O_5(OH)]_2$	~5.2	~9.0	variable	-	-	
Bramallite	$(M^+,H_2O)_x[Al,Mg,Fe)(Si,Al)_2O_5(OH)]_2$	-	-	-	-	-	
Hydromica	$(M^+,H_2O)_x[Al(Si,Al)_2O_5(OH)]_2$	-	-	-	-	-	
*Illite	$(M^+,H_2O)_x[Al,Mg,Fe)(Si,Al)_2O_5(OH)]_2$	5.2	9.0	9.95	95.5	C2/c	
Goldichite	$K_2[Fe^{3+}_2(SO_4)_4(H_2O)_4]\cdot 4H_2O$	10.387(6)	10.486(6)	9.086(5)	101.68(7)	P2,/c	(5)

Ref.: (1) Mereiter (1974). (2) Moore et al. (1976). (3) Moore (1975). (4) Moore and Araki (1972). (5) Graeber and Rosenzweig (1971). (6) Ya-hsien et al. (1963). (7) Wardle and Brindley (1972). (8) Bailey (1980). (9) Guggenheim and Bailey (1975).

$\gamma = 91.03(2)$, $\gamma = 89.75(2)^o$

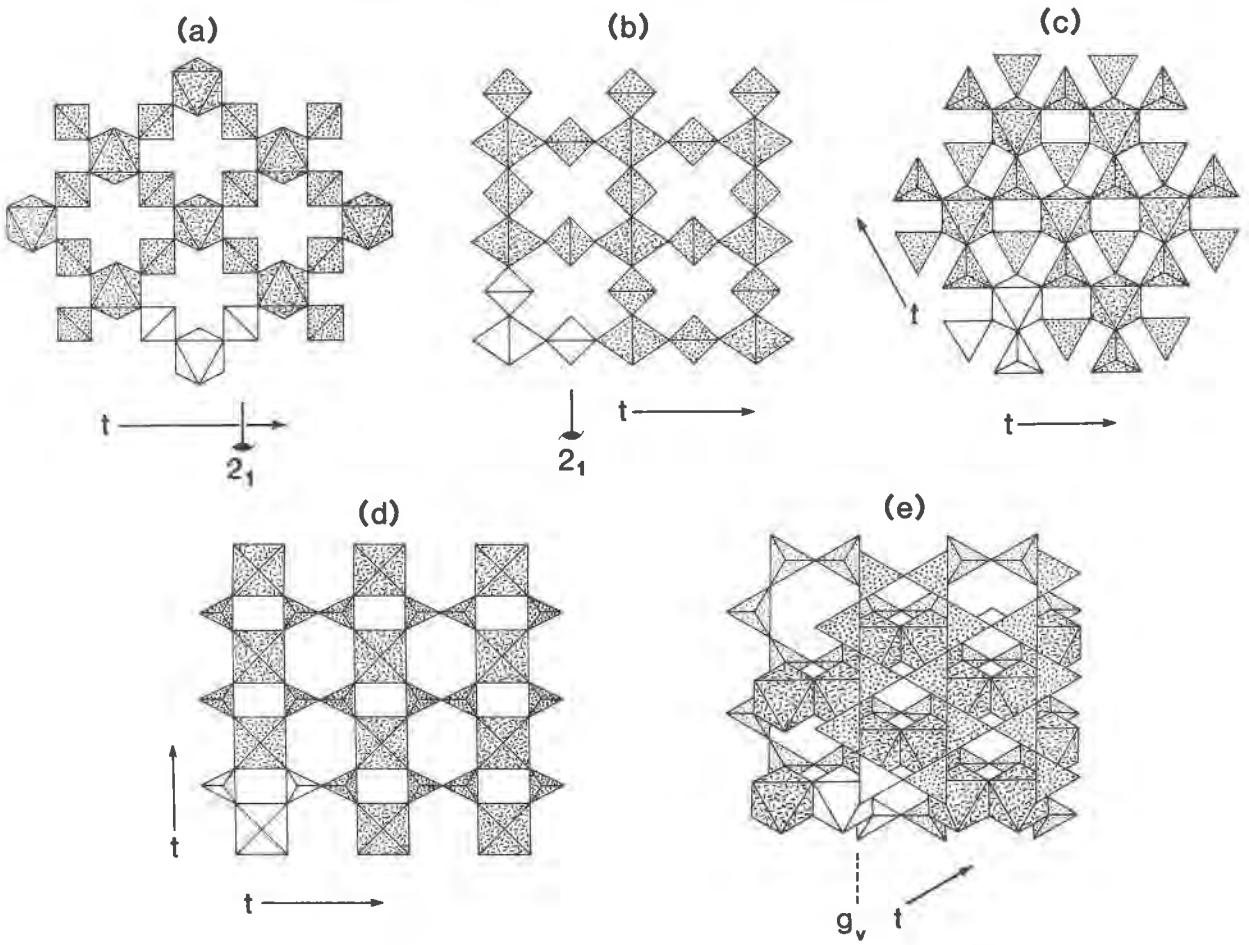

Fig. 9. Infinite $[M(TO_4)_2\Phi_n]$ sheets found in minerals: (a) $[M(TO_4)_2\Phi_2]$ = rhomboclase-type; (b) $[M(TO_4)_2\Phi_2]$ = olmsteadite-type; (c) $[M(TO_4)_2]$ = merwinite-type; (d) $[M(T_2O_7)\Phi_2]$ = bafertisite-type; (e) $[M(T_2O_5)\Phi]$ = muscovite-type. The fundamental $[M(TO_4)_2\Phi_4]$ cluster is unshaded, and the repetition operators are shown.

peated with corner-sharing between octahedra, and the resultant sheet is repeated with corner-sharing between tetrahedra. In rosenbuschite, the basic cluster is the $[M_4(TO_4)_8\Phi_8]$ cluster that is repeated by simple trans-

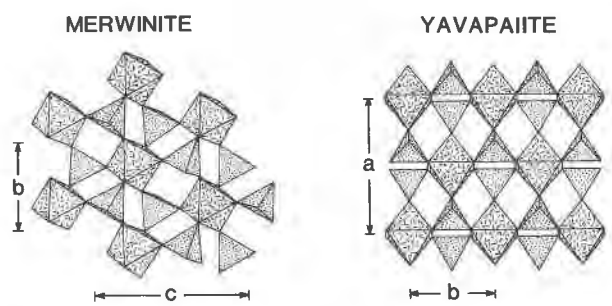

Fig. 10. The structures of merwinite (left) and yavapaiite (right), based on the $[M(TO_4)_2]$ sheet (Fig. 9c); adjacent chains are linked by [8]-and [10]-coordinated Ca and K respectively.

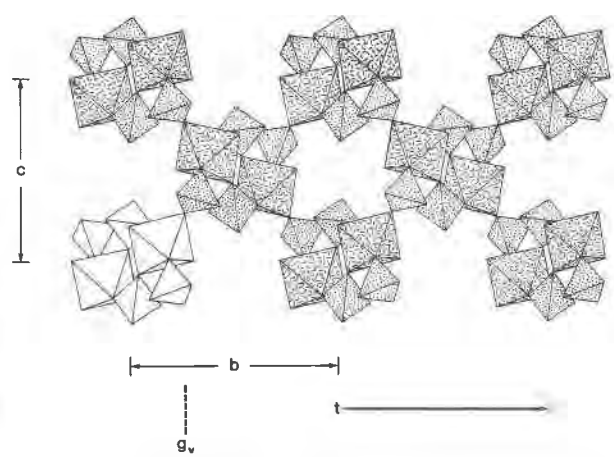

Fig. 11. The structure of goldichite, a very thick corner-linked sheet of $[M_2(TO_4)_4\Phi_6]$ clusters, one of which is unshaded in this diagram; adjacent layers are linked by [9]-coordinated K and a network of hydrogen-bonds.

Table 8. $MT_2\Phi_n$ minerals based on infinite frameworks

Mineral	Formula	a(Å)	b(Å)	c(Å)	α(°)	β(°)	γ(°)	S.G.	Ref.
Keldyshite	$(Na,H_3O)[ZrSi_2O_7]$	9.0(1)	5.34(2)	6.96(3)	92(1)	116(1)	88(1)	$P\bar{1}$	(1)
Parakeldyshite	$Na[ZrSi_2O_7]$	9.31	5.42	6.66	94.3	115.3	89.6	$P\bar{1}$	(1)
Nenadkevichite	$Na_2[NbSi_2O_6(OH)]\cdot 2H_2O$	7.408(2)	14.198(3)	7.148(2)				Pbam	(2)
Labuntsovite	$K_2[TiSi_2O_6(OH)]\cdot 2H_2O$	14.18	13.70	7.74		117		C2/m	(3)
Batisite	$Na_2Ba[TiSi_2O_6O]_2$	10.40	13.85	8.10				Ima2	(4)
Shcherbakovite	$K_2Ba[(Ti,Nb)Si_2O_6O]_2$	10.55	13.92	8.10				Ima2	
Alkali pyroxenes	$M^+[M^{3+}Si_2O_6]$	~9.7	~8.8	~5.25		~107.5		C2/c	(5)
Calcic pyroxenes	$Ca[M^{2+}Si_2O_6]$	~9.8	~8.9	~5.24		~105.5		C2/c	(5)
Låvenite	$(Na,Ca)_3[ZrSi_2O_7O]F$	10.83(1)	9.98(1)	7.174(5)		108.1(1)		$P2_1/a$	(6)
Wöhlerite	$Na_2Ca_4[ZrNb(Si_2O_7)_2O_2]F$	10.823(3)	10.244(3)	7.290(2)		109.00(4)		$P2_1$	(7)
Rosenbuschite	$(Ca,Na)_2[Zr_2Ti_2(Si_2O_7)_4O_2F_2]F_4$	10.12(5)	11.29(5)	7.27(3)	91.3(5)	99.7(5)	111.8(5)	$P\bar{1}$	(8)

References: *(1) Khalilov et al. (1977). (2) Perrault et al. (1973). (3) Golovastikov (1974). (4) Nikitin and Belov (1962). (5) Cameron and Papike (1981). (6) Mellini (1981). (7) Mellini and Merlino (1979). (8) Shibaeva et al. (1964).*

lation in all three dimensions, with M–T and T–T corner-sharing. Thus the progressive increase in complexity of the basic clusters in these three structures is accompanied by increasing condensation of the component polyhedra.

Structural trends

Brown (1981) has introduced a structure-based scale of Lewis acid and base strength that can be used, together with some of the ideas introduced here, to provide considerable insight into aspects of structure type that have hitherto been difficult to approach. The Lewis acid strength of a cation is defined as its valence divided by its *average* coordination number; it is thus the average bond-valence of a characteristic bond formed by that cation, and Brown (1981) lists values for numerous cations. The Lewis base strength of an anion is analogously defined as the characteristic valence of a bond formed by the anion. Simple anions can show a considerable range of bond-valence, but this is generally greatly reduced for complex anions. As an example, consider thenardite, Na_2SO_4. The bond-valences to the oxygen anion vary from ~0.16 v.u. for Na–O to ~1.5 v.u. for S–O. Now consider the oxyanion $(SO_4)^{2-}$; the S–O bond has a bond-valence of ~1.5 v.u., leaving ~0.5 v.u. per oxygen to be satisfied by 3 additional bonds (assuming an average coordination number of [4] for oxygen). Thus the Lewis base strength of the $(SO_4)^{2-}$ oxyanion is 0.5/3 = 0.17 v.u. Obviously this value is to some

Table 9. Definition of structural units

Complex anion: a cation surrounded by a coordination polyhedron of anions such that the aggregate formal change is negative; e.g. $(SO_4)^{2-}$, $(SiO_4)^{4-}$.

Homopolyhedral cluster: a cluster of similar coordination polyhedra bonded together.

Heteropolyhedral cluster: a cluster of more than one type of coordination polyhedra bonded together.

Fundamental building block (FBB): the homo- or heteropolyhedral cluster that is repeated by the (translational) symmetry operators of the structure to form the strongly bonded part of the structure.

Structure Module: the strongly bonded part of the structure that is formed by repetition/polymerization of the polyhedral cluster that forms the FBB of the structure.

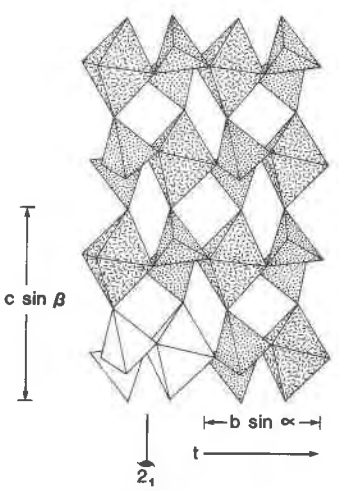

Fig. 12. The structure of keldyshite, based on a $[ZrSi_2O_7]$ framework; the fundamental $[M(TO_4)_2\Phi_4]$ is shown unshaded, and the repetition operators are shown; the repetition operator (not shown) orthogonal to the diagram is a simple translation.

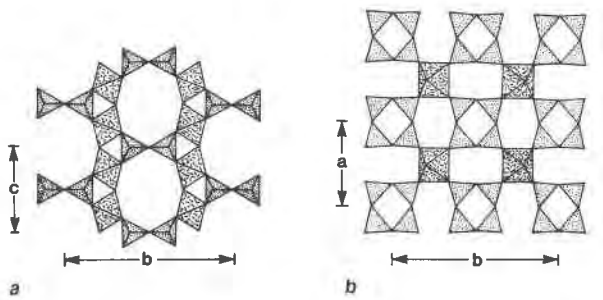

Fig. 13. The structure of nenadkevichite: (a) shows tancoite-type chains ‖c, cross-linked by corner-sharing between tetrahedra to form pyro-groups; (b) shows linkage of tancoite-type chains in the two directions orthogonal to their length, with the 4-membered Si_4O_{12} rings cross-linking chains.

extent sensitive to the average coordination number assumed for oxygen; the value [4] is usually adequate, and it is generally obvious when another value is more appropriate. Brown (1981) also lists Lewis basicity values for numerous oxyanions; these values can easily be calculated as indicated above.

Consider now the hypothesis of Hawthorne (1983a). In terms of Lewis acid and base strengths, it considers the polymerization of the most tightly-bonded oxyanions in the structure. Increasing polymerization of these oxyanions will decrease their resultant Lewis base strength. This suggests that the degree of polymerization in these structures should be related to the average Lewis base strength of their component oxyanions, i.e. the Lewis base strength of $[(MO_6^{2-}) + 2(TO_4^{2-})]$ in the structures considered here. This premise is examined in Figure 16; there is a general trend of increasing polymerization (condensation) with increasing Lewis base strength of the component oxyanions. Furthermore, minerals lying close to the average trend line tend to be more common (alum and halotrichite groups, kröhnkite, talmessite and brackebuschite groups, the dioctahedral micas and the monoclinic pyroxenes) than those that lie far off the trend (fleischerite group, ransomite and krausite, and the titanium-niobium silicates). Considering the generality of the problem, this result is quite encouraging; it will be interesting to see if this type of relationship holds for other $M_xT_y\Phi_z$ stoichiometries.

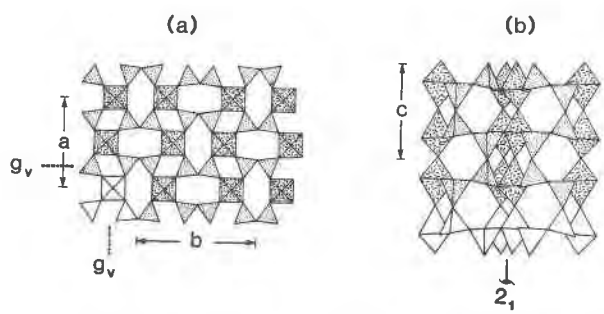

Fig. 14. The structure of batisite: (a) the basic $[M(TO_4)_2\Phi_4]$ cluster (unshaded) is repeated by glide and screw operators to form a sheet; (b) this sheet is repeated by a 2_1 screw operator to form a framework.

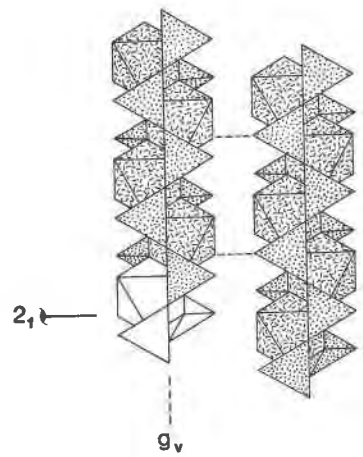

Fig. 15. The pyroxene structure as a framework structure; the basic $[M(TO_4)_2\Phi_4]$ cluster is unshaded, and is repeated by 2_1 screw and vertical glide operators in the plane of the diagram, and by a translation operator orthogonal to the plane of the diagram.

Inter-module linkage

Translational symmetry operators repeat the fundamental building block to form a three-dimensional array that may be connected in 0, 1, 2 or 3 dimensions. Let us define this array as the *structure module*. So far, this scheme has exploited the strong intra-module linkage and has focussed solely on this aspect of structures. However, by going one step further, we can get insight into the extra-module linkage, that is the weak bonding between the structure module and the low-valence charge-balancing cations.

The definitions of Lewis acid and base strength outlined

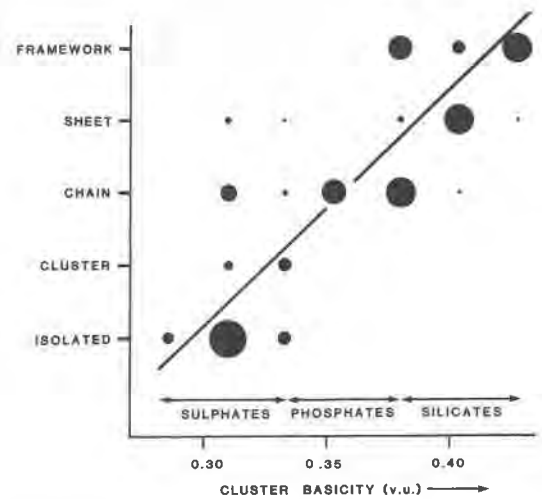

Fig. 16. Structure type as a function of the Lewis basicity of the component oxyanions $[(MO_6^{2-}) + 2(TO_4^{2-})]$; the size of the circles is proportional to the number of species with that particular basicity and structure type.

earlier lead to the valence matching principle (Brown, 1981), which states that the most stable structures will be formed when the Lewis acid strength of the cation is most nearly equal to the Lewis base strength of the anion. This principle may be exploited in this instance by considering the principal module of a structure as a (very complex) oxyanion. The Lewis basicity of the module may be calculated, and through the valence matching principle, may be related to the Lewis acidity of the weakly-bonding cations in the structure. This provides an insight and even some predictive capability with regard to the identity and coordination number of these weakly-bonding cations.

Graphical isomers (Hawthorne, 1984) have the same Lewis basicity (assuming the same type of cations); inspection of actual structures indicates that this is not chemically realistic. This difference can be traced to variation in anion type, and can be naturally handled by including hydrogen (as OH or H_2O) as a component of the structure module in the following way. If the bond-valence contributed to the anion is less than 0.67 v.u., the anion is considered to be H_2O; it is bonded to no more cations, and forms two hydrogen-bonds. If the bond-valence contributed to the anion falls between 0.67 and 1.00 v.u. (and the anion is not bonded to a tetrahedrally coordinated cation), the anion is considered to be OH; it is assumed to form no additional bonds to other cations (this is not always valid of course). It should be noted that this scheme invariably reproduces the anion type of the structure module; the validity of this procedure stems from the valence-sum rule (Brown, 1981), which is closely related to Pauling's second rule (Pauling, 1960).

Calculation of module basicity hinges on the use of the most appropriate anion coordination numbers. In the absence of a systematic study of anion coordination numbers in these structures, the following approximation is used: when O^{2-} is bonded to M^{3+} and T^{6+}, the assigned CN is 3; at all other times it is 4, except when H is involved (see above).

According to the valence matching principle, the module basicity should approximately match the linking cation acidity; thus the linking cation may be predicted on this basis. The cation coordination number may be predicted from the number of bonds required for the simple anions of the module to attain their ideal coordination numbers (of [3] or [4]), divided by the number of linking non-module cations. The actual acidity of the linking cation can (and frequently does) depart from its ideal (average) value. The value of a cation's acidity in an actual structure is equal to its formal charge divided by the number of bonds it forms to the module. This number of bonds is equal to the conventional coordination number, except for structures in which there are non-module nonzeolitic H_2O molecules. To appreciate the effect of such H_2O molecules, consider the bond-valence structure around the oxygen atom (Fig. 17). The bond-valence requirements of the oxygen are satisfied by a cation–anion bond of valence less than or equal to ~0.5 v.u., together with two short O–H bonds of valence greater than or equal to ~0.75 v.u. To satisfy the

Fig. 17. Bond-valence structure of H_2O bonded to [6]-coordinate divalent and trivalent cations.

bond-valence requirements around each hydrogen atom, each hydrogen forms at least one hydrogen bond with neighboring anions. Thus the H_2O molecule is acting as a bond-valence transformer, causing one stronger bond to be split into (at least) two weaker bonds. The presence of non-module H_2O in the structure increases the number of bonds from the charge-balancing cation(s) to the module, and decreases the valence of these bonds; this increases the effective coordination number of the charge-balancing cation (defined as the number of bonds formed to the structure module), and decreases its effective Lewis acidity. Note that all of the H_2O molecules need not be bonded directly to the cations, so this transformer action can also function entirely through hydrogen bonds (e.g., halotrichite group minerals).

As an example, consider the structure of botryogen (Table 6 and Fig. 2e). The module formula is $[Fe_2^{3+}(SO_4)_4(OH)_2(H_2O)_2]^{4-}$; the oxygen atoms bonded to Fe^{3+} and S have an assigned (and observed) coordination number [3], the hydroxyl and water oxygens are assumed to be satisfied, with two hydrogen bonds emanating from each H_2O anion; the remaining oxygens have an assigned coordination number [4]. The number of bonds needed to satisfy these anion coordination number requirements is $2 \times 10 + 6 \times 1 - 4 = 22$; the -4 term refers to the four hydrogen bonds emanating from the H_2O anions. The total bond-valence needed to satisfy the valence-sum rule in the module is $(2 - t)10 + (2 - t - o)6 - 4h = 32 - 16t - 6o - 4h$, where t, o and h are the tetrahedral (1.5), octahedral (0.5) and hydrogen (0.25) bond-valences respectively. The module basicity is $(32 - 16t - 6o - 4h)/22 = 0.18$ v.u. and the module charge is 4^-. The number of bonds to the module from the linking cations is 22 and the charge of the linking cations is 4^+; this indicates a monovalent cation coordination number of $22/4 \sim [6]$ and a divalent cation coordination number of $22/2 = [11]$. Thus we predict a cation acidity of 0.18 v.u. and cation coordination numbers of $[6]^+$ and $[11]^{2+}$. In botryogen, the module charge of 4^- is balanced by the presence of 2Mg, with an ideal Lewis acidity of 0.36 v.u. (Brown, 1981). However, there are five waters of hydration for each Mg, and thus the anion coordination of Mg is $(H_2O)_5O$; each water anion functions as a bond-valence transformer, giving the Mg an effective coordination number (i.e. number of bonds to the structure module) of $5 \times 2 + 1 = [11]$, and a (modified) actual acidity of $2/11 = 0.18$ v.u., both values in agreement with predictions. This scheme thus provides an explanation as to why botryogen is hydrated, and in fact would predict that botryogen would be hydrated, given the module part of the structure and the identity of the charge-balancing cation.

Isolated polyhedra structures

The $[M^{3+}(T^{6+}O_4)_2(H_2O)_6]^-$ cluster has a basicity of 0.08 v.u. and a predicted monovalent cation coordination number of [12]. For amarillite, both the ideal and observed cation acidities are 0.16 v.u. and the observed cation coordination number is [6]. These values are significantly different from the calculated values, suggesting that higher hydrates should be quite stable, and indeed this is the case, with members of the mendozite and alum groups showing good agreement with predicted values (Table 10). This cluster has a predicted divalent cation coordination of [24] and a predicted cation acidity of 0.08 v.u. No individual cation has these characteristics, but they may be attained by high degrees of hydration through the transformer action of the H_2O anion. In the members of the halotrichite group (Tables 1 and 10), the divalent cations have nominal acidities of 0.36–0.40 v.u. and nominal coordination numbers of [6]. However, the divalent cation is coordinated by six (H_2O) anions, and thus twelve hydrogen-bonds emanate from this group. These are further split by the hydrogen-bonding network of the additional four H_2O anions to form twenty bonds to the module. Thus the divalent cation has an effective coordination number of [20] and an actual acidity of 2/20 = 0.10 v.u., in good agreement with the predicted values. This provides an adequate explanation for the high degrees of hydration in some of these minerals, the hydrogen-bonding network reducing the effective Lewis acidity of the cation and bringing it into a reasonable match with the Lewis basicity of the structure module. The situation is similar in aubertite, except for the additional Cl that balances one of the charges of the Cu^{2+} cations.

The minerals of the picromerite group are based on the $[M^{2+}(T^{6+}O_4)_2(H_2O)_6]^{2-}$ module, with a basicity of 0.13 v.u. (Table 10) and predicted cation coordination numbers of [10] and [20] for monovalent and divalent cations respectively. The observed cation acidities and coordination numbers are in good agreement with these values, although highly hydrated divalent cation equivalents should also be possible.

Table 10. Basicities, acidities (v.u.) and cation coordination numbers (CN) in the isolated polyhedra structures

	module basicity	predicted CN	module charge	nominal acidity[1]	actual acidity[2]	observed CN[3]
Amarillite	0.08	12	1^-	0.16	0.16	6
Mendozite	0.08	12	1^-	0.16	0.09	11
Kalinite	0.08	12	1^-	0.13	0.09	11
Sodium alum	0.08	12	1^-	0.16	0.08	12
Potassium alum	0.08	12	1^-	0.13	0.08	12
Halotrichite	0.08	24	2^-	0.36	0.05	20
Aubertite	0.13	15	2^-	0.45	0.12	17
Picromerite	0.13	10	2^-	0.13	0.13	8
Fleischerite	0.17	10	6^-	~0.2	0.20	10
Despujolsite	0.17	10	6^-	0.29	0.20	10

[1]*quoted acidity of cation.* [2]*actual acidity of cation in structure.* [3]*given as the number of bonds to the module from the cation.*

Table 11. Basicities, acidities (v.u.) and cation coordination numbers (CN) in the finite cluster structures

	module basicity	predicted CN	module charge	nominal acidity	actual acidity	observed CN
Anapaite	0.29	7	4^-	0.29	0.29	7
Bloedite	0.14	7	2^-	0.16	0.14	8
Leonite	0.14	7	2^-	0.13	0.14	8
Schertelite	0.25	6	2^-	0.25	0.20	5
Roemerite	0.08	18	2^-	0.36	0.18	12
Metavoltine	0.12	9	10^-	0.18	0.14	8

The $[M^{4+}(T^{6+}O_4)_2(OH)_6]^{6-}$ module is the basis of the minerals of the fleischerite group, with a basicity of 0.17 v.u. and predicted coordination numbers of [5] and [10] for monovalent and divalent cations respectively. Brown (1981) does not give a Lewis basicity for Pb^{2+}, but the value will be ~0.2 v.u. (Table 10). Again the observed values are in reasonably good agreement with the predicted values.

Finite cluster structures

Anapaite, bloedite and leonite show good agreement with the predicted values of cation acidity and coordination number (Table 11). Schertelite is an interesting example: the presence of acid phosphate groups modifies the bond-valences in the phosphate group to 1.0 to the OH anion and 1.33 v.u. to each of the remaining three oxygens. The resultant module basicity is 0.25 v.u. with a predicted cation coordination of [6]. Ammonium $(NH_4)^+$ is a complex cation with an ideal acidity of (5–4)/4 = 0.25 v.u.; in schertelite, there is one bifurcated hydrogen-bond, and thus the actual cation acidity is 0.20 v.u. with an observed coordination number of [5], in reasonable agreement with the predicted values (Table 11). The agreement for roemerite is not good; the calculated module basicity and predicted cation coordination number suggests that a more hydrated form (with ~$10H_2O$) would occur. The agreement for metavoltine is good, particularly so in view of the complexity of the structure; although only average values can be predicted, these agree well with the average values of cation acidity and coordination number observed in the actual structure.

Chain structures

Minerals of the kröhnkite, talmessite and fairfieldite groups (Table 3) all show close agreement with predicted cation acidities and coordination numbers (Table 12). For tancoite (Table 4), the additional hydrogen was included in the module basicity calculation, and the average of the observed values for cation acidity and coordination agree well with the predicted values. The agreement for the jahnsite and segelerite groups is reasonable, considering the complexity of the structures; it is apparent that the high

Table 12. Basicities, acidities (v.u.) and cation coordination numbers (CN) in the chain structures

	module basicity	predicted CN	module charge	nominal acidity	actual acidity	observed CN
Kröhnkite	0.13	8	2^-	0.16	0.14	7
Brandtite	0.25	8	4^-	0.29	0.29	7
Tancoite	0.17	7	3^-	0.18	0.15	7
Sideronatrite	0.17	6	2^-	0.16	-	-
Jahnsite	0.20	10	4^-	0.34	0.25	9
Guildite	0.13	15	2^-	0.45	0.20	10
Yftisite	0.30	10	6^-	-	0.38	8
Brackebuschite	0.24	9	4^-	~0.2	0.25	8
Goedkenite	0.22	10	4^-	0.24	-	-
Fornacite	0.18	11	4^-	~0.2	0.20	10
Tornebohmite	0.30	10	6^-	-	0.30	10
Ransomite	0.08	24	2^-	0.45	0.20	10
Krausite	0.08	12	1^-	0.13	0.10	10
Botryogen	0.18	11	4^-	0.36	0.18	11

hydration states in these minerals are necessary to reduce the ideal cation acidities and bring them more into line with the predicted values. There is some discrepancy for guildite, in which the actual cation acidity is larger than the module basicity; the same situation occurs for ransomite (Table 12), as well as roemerite and amarillite, and suggests that the method of handling anion coordination number is not yet quite adequate for the $[M^{3+}(T^{6+}O_4)\Phi_n]$ modules linked by divalent cations.

For the brackebuschite, fornacite and vauquelinite groups (Table 5), the calculations are in good agreement with the observed data, correctly predicting the identities of the linking cations (Pb^{2+}, Sr^{2+}) and their high ([9]–[11]) coordination numbers, as compared for example with the talmessite and fairfieldite groups, with Ca as the linking cation and observed coordination numbers of [7]. Krausite and botryogen show good agreement (Table 12). It is curious that the very complex botryogen and metavoltine structures show good agreement with these calculations, whereas the simpler $M^{3+}T^{6+}$ structures (ransomite, guildite, etc.) do not; perhaps it is of significance that the former are reasonably common minerals, wheras the latter are rare.

Sheet structures

Rhomboclase is another $M^{3+}T^{6+}$ structure which shows some discrepancy between observed and predicted values. The assignment of this disagreement to inadequate anion coordination assignment is also suggested by the fact that the agreement for olmsteadite (Table 13), whose structure module is a geometrical isomer of that of rhomboclase, is very good. The values for merwinite are not well-predicted, but it should be noted that the Ca coordinations in the observed structure do have strong octahedral affinities. The

Table 13. Basicities, acidities (v.u.) and cation coordination numbers (CN) in the sheet structures

	module basicity	predicted CN	module charge	nominal acidity	actual acidity	observed CN
Rhomboclase	0.13	8	1^-	0.25	0.20	5
Olmsteadite	0.23	9	5^-	0.28	0.23	7
Merwinite	0.33	6	6^-	0.29	0.25	8
Brianite	0.22	8	4^-	0.20	-	-
Yavapaite	0.08	12	1^-	0.13	0.10	10
Bafertisite	0.27	7	5^-	0.31	0.29	7
Muscovite	0.15	7	1^-	0.13	0.13	8
Goldichite	0.08	12	1^-	0.13	0.09	11

values for the remaining structures (Table 13), including the dioctahedral micas, are good; this is particularly notable for bafertisite, in which the low observed mean cation coordination number of [7] is successfully forecast.

Framework structures

Predicted and observed values for the framework structures are given in Table 14. There is good agreement between predicted and actual values, a fact that is particularly encouraging considering the complexity of such minerals as låvenite, wöhlerite and rosenbuschite.

Mineral solubility

In water, the intermolecular bonds will have the valence structure illustrated in Figure 18 (Brown, 1981). The hydrogen atoms have a Lewis acid strength of 0.2 v.u. and the oxygen atoms have a Lewis base strength of 0.2 v.u., assuming a CN = [4] for oxygen. Hence water forms an acid-base network that can react with other acid-base compounds of suitable strength. Minerals in which the base strength of the structure module matches the acid strength of water and the base strength of water matches the acid strength of the extra-module cation are generally soluble,

Table 14. Basicities, acidities (v.u.) and cation coordination numbers (CN) in the framework structures

	module basicity	predicted CN	module charge	nominal acidity	actual acidity	observed CN
Keldyshite	0.14	7	1^-	0.13	0.13	8
Nenadkevichite	0.06	13	2^-	0.13	0.09	11
Batisite	0.11	10	4^-	0.17	0.13	10
Calcic pyroxene	0.22	10	2^-	0.29	0.25	8
Sodic pyroxene	0.17	8	1^-	0.16	0.17	8
Låvenite	0.23	8	5^-	0.27	0.24	8
Wöhlerite	0.23	7	10^-	0.25	0.24	7
Rosenbuschite	0.23	7	10^-	0.23	0.24	6

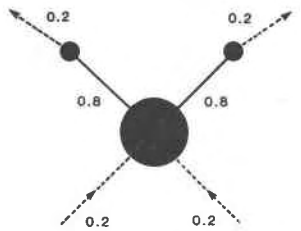

Fig. 18. The bond-valence structure of liquid water (from Brown, 1981).

provided that the module is not infinite in three-dimensions. This is because the acid and base components will, according to the valence matching principle, form an equally good or even better match with the water than they do with each other. Minerals whose module basicities and cation acidities are much greater than 0.2 v.u. will be insoluble, as they can form a better match with each other than they can with water. A qualitative survey of the minerals discussed here shows this to be the case. All of the isolated polyhedra minerals of Table 1 are soluble, with the possible exception of those of the fleischerite group. Of the finite cluster minerals (Table 2), anapaite is insoluble (relatively) while the rest are soluble. In the chain structures (Tables 3, 4 and 5), predictions work particularly well. In the kröhnkite (module basicity = 0.13, observed cation acitity = 0.16 v.u.) is soluble where the isostructural minerals roselite and brandtite (module basicity = 0.25, observed cation acidity = 0.29 v.u.) are insoluble; the talmessite and fairfieldite group minerals are likewise insoluble. In the tancoite-type chain minerals, sideronatrite is soluble; data are not available for most of the other minerals, but tancoite and guildite are predicted to be soluble, with the rest insoluble. The brackebuschite minerals of Table 5 are expected to be insoluble, and the complex chain minerals of Table 6 are expected to be soluble; available data bear out these predictions.

It would be of interest to put these qualitative predictions on to a more quantitative basis. For example, one might expect the solubility of a mineral to depend quantitatively on both its module basicity and the degree of mismatch between the module basicity and the nominal cation acidity. Unfortunately there is very little quantitative solubility data for the minerals discussed here, and so general trends between different structure types cannot be examined in detail.

Summary

1. It is proposed that *mineral structures may be ordered or classified according to the polymerization of those cation coordination polyhedra of higher bond-valences.*

2. Higher bond-valence polyhedra bond together to form *homo-* or *heteropolyhedral clusters* that constitute the *fundamental building block* (FBB) of the structure.

3. The FBB is repeated (often polymerized) by translational symmetry operators to form the *structure module*, a complex anionic polyhedral array (not necessarily connected) whose excess charge is balanced by the presence of (linking) large low-valence cations.

4. The Lewis basicity of the structure module should approximately match the Lewis acidity of the charge-balancing cations for the structure to be stable.

These four points form the basis of a method of structural classification of minerals, which has been applied to a broad group of sulphates, chromates, phosphates, arsenates, vanadates and silicates with the general stoichiometry $MT_2\Phi_n$ (M = octahedrally coordinated cations, T = tetrahedrally coordinated cations, Φ = unspecified anions). In addition to its applicability to a wide variety of minerals, this scheme has the additional advantage that the nature of its formulation allows rationalization and prediction of such features as large low valence cation type, large cation coordination, the degree of hydration of minerals, and their relative solubilities in water.

Acknowledgments

Financial support during this work was provided by the Natural Sciences and Engineering Research Council of Canada in the form of a fellowship and a grant to the author. I would like to thank Robert M. Hazen, Paul B. Moore and Malcolm Ross for their reviews.

References

Andersen, S. (1981) The description of complex alloy structures. In M. O'Keefe and A. Navrotsky, Eds., Structure and Bonding in Crystals, II, p. 233–258. Academic Press, New York.

Andersen, S. and Hyde, B. G. (1982) An attempted exact, systematic, geometrical description of crystal structures. Zeitschrift für Kristallographie, 158, 119–131.

Bailey, S. W. (1980) Structures of layer silicates. In G. W. Brindley and G. Brown, Eds., Crystal Structures of Clay Minerals and their X-ray Identification, p. 1–123. Mineralogical Society, London.

Balko, V. P. and Bakakin, V. V. (1975) The crystal structure of the natural yttrium and rare-earth fluortitano-silicate $(Y,Tr)_4(F,OH)_6TiO(SiO_4)_2$ (Yftisite). Zhurnal Strukturnoi Khimii, 16, 837–842.

Bragg, W. L. (1930) The structure of silicates. Zeitschrift für Kristallographie, 74, 237–305.

Brotherton, P. D., Maslen, E. N., Pryce, M. W. and White, A. H. (1974) Crystal structure of collinsite. Australian Journal of Chemistry, 27, 653–656.

Brown, I. D. (1981) The bond-valence method: an empirical approach to chemical structure and bonding. In M. O'Keeffe and A. Navrotsky, Eds., Structure and Bonding in Crystals, II, p. 1–30. Academic Press, New York.

Bukin, V. I. and Nozik, Yu. Z. (1975) Neutron-diffraction study of the crystal structure of cobalt astrakhanite $Na_2Co(SO_4)_2 \cdot 4H_2O$. Soviet Physics Crystallography, 20, 180–182.

Cameron, M. and Papike, J. J. (1981) Structural and chemical variations in pyroxenes. American Mineralogist, 66, 1–50.

Carapezza, M. and Riva di Sanseverino, L. (1968) Crystallography and genesis of double sulfates and their hydrates. II. Structure, powder pattern and thermoanalysis of cyanochoite, $K_2Cu(SO_4)_2 \cdot 6H_2O$. Mineralogia Petrologia Acta, 14, 23–37.

Carapezza, M. and Riva di Sanseverino, L. (1970) Crystallography and genesis of double sulfates and their hydrates. III. Picromerite, $K_2Mg(SO_4)_2 \cdot 6H_2O$: a methodological check. Mineralogia Petrologia Acta, 16, 5–11.

Catti, M., Ferraris, G. and Ivaldi, G. (1977) Hydrogen bonding in the crystalline state. Structure of talmessite, $Ca_2(Mg,Co)(AsO_4)_2 \cdot 2H_2O$, and crystal chemistry of related minerals. Bulletin de la Société francaise de Minéralogie et de Cristallographie, 100, 230–236.

Catti, M., Ferraris, G. and Ivaldi, G. (1979) Refinement of the crystal structure of anapaite, $Ca_2Fe(PO_4)_2 \cdot 4H_2O$: hydrogen bonding and relationships with the bihydrated phase. Bulletin de la Société francaise de Minéralogie et de Cristallographie, 102, 314–318.

Christ, C. L. (1960) Crystal chemistry and systematic classification of hydrated borate minerals. American Mineralogist, 45, 334–340.

Christ, C. L. and Clark, J. R. (1977) A crystal-chemical classification of borate structures with emphasis on hydrated borates. Physics and Chemistry of Minerals, 2, 59–87.

Cocco, G., Fanfani, L. and Zanazzi, P. F. (1967) The crystal structure of fornacite. Zeitschrift für Kristallographie, 124, 385–397.

Cromer, D. T., Kay, M. I. and Larson, A. C. (1967) Refinement of the alum structures. II. X-ray and neutron diffraction of $NaAl(SO_4)_2 \cdot 12H_2O$, γ-alum. Acta Crystallographica, 22, 182–187.

Donaldson, D. M. and Barnes, W. H. (1955) The structures of the minerals of the descloizite and adelite groups: III-brackebuschite. American Mineralogist, 40, 597–613.

Fanfani, L. and Zanazzi, P. F. (1968) The crystal structure of vauquelinite and the relationship to fornacite. Zeitschrift für Kristallographie, 126, 433–443.

Fanfani, L. and Zanazzi, P. F. (1969) Structural similarities of some secondary lead minerals. Mineralogical Magazine, 31, 522–529.

Fanfani, L., Nunzi, A. and Zanazzi, P. F. (1970a) The crystal structure of roemerite. American Mineralogist, 55, 78–89.

Fanfani, L., Nunzi, A. and Zanazzi, P. F. (1970b) The crystal structure of fairfieldite. Acta Crystallographica, B26, 640–645.

Fang, J. H. and Robinson, P. D. (1972) Crystal structures and mineral chemistry of double-salt hydrates: II. The crystal structure of mendozite, $NaAl(SO_4)_2 \cdot 11H_2O$. American Mineralogist, 57, 1081–1088.

Ferraiolo, J. A. (1982) A systematic classification of nonsilicate minerals. Bulletin of the American Museum of Natural History, 172, 1–237.

Giacovazzo, G., Scordari, F., Todisco, A. and Menchetti, S. (1976) Crystal structure model for metavoltine from Sierra Gorda. Tschermaks Mineralogische und Petrographische Mitteilungen, 23, 155–165.

Ginderow, D. and Cesbron, F. (1979) Structure cristalline de l'aubertite, $AlCuCl(SO_4)_2 \cdot 14H_2O$. Acta Crystallographica, B35, 2499–2502.

Golovastikov, N. I. (1974) Crystal structure of the alkali titanosilicate labuntsovite. Soviet Physics Crystallography, 18, 596–599.

Graeber, E. J., Morosin, B. and Rosenzweig, A. (1965) The crystal structure of krausite, $KFe(SO_4)_2 \cdot H_2O$. American Mineralogist, 50, 1929–1936.

Graeber, E. J. and Rosenzweig, A. (1971) The crystal structures of yavapaiite, $KFe(SO_4)_2$, and goldichite, $KFe(SO_4)_2 \cdot 4H_2O$. American Mineralogist 56, 1917–1933.

Guggenheim, S. and Bailey, S. W. (1975) Refinement of the margarite structure in subgroup symmetry. American Mineralogist, 60, 1023–1029.

Hawthorne, F. C. (1979) The crystal structure of morinite. Canadian Mineralogist, 17, 93–102.

Hawthorne, F. C. (1983a) Graphical enumeration of polyhedral clusters. Acta Crystallographica, A39, 724–736.

Hawthorne, F. C. (1983b) The crystal structure of tancoite. Tschermaks Mineralogische und Petrographische Mitteilungen, 31, 121–135.

Hawthorne, F. C. (1984) The crystal structure of stenonite, and the classification of the aluminofluoride minerals. Canadian Mineralogist, 22, 245–251.

Hawthorne, F. C. and Ferguson, R. B. (1975) Refinement of the crystal structure of kröhnkite. Acta Crystallographica, B31, 1753–1755.

Hawthorne, F. C. and Ferguson, R. B. (1977) The crystal structure of roselite. Canadian Mineralogist, 15, 36–42.

Hellner, E. (1984) Frameworks and a classification scheme for inorganic and intermetallic structure types. Thirteenth International Congress of Crystallography, Collected Abstracts, p. C–214.

Hofmeister, W. and Tillmanns, E. (1978) Strukturelle Untersuchungen an Arsenbrackebuschit. Tschermaks Mineralogische und Petrographische Mitteilungen, 25, 153–163.

Hulliger, F. (1981) On polycompounds: polycationic and polyanionic tetrelides, pnictides, and chalcogenides. In M. O'Keefe and A. Navrotsky, Eds., Structure and Bonding in Crystals, II, p. 297–352. Academic Press, New York.

Khalilov, A. D., Khomiakov, A. P. and Makhmudov, S. A. (1977) Crystal structure of keldyshite, $NaZr(Si_2O_6OH)$. Doklady Akademii Nauk SSSR, 238, 573–577.

Khan, A. A. and Baur, W. H. (1972) Salt hydrates. VIII. The crystal structure of sodium ammonium orthochromate dihydrate and magnesium diammonium bis(hydrogen orthophosphate) tetrahydrate and a discussion of the ammonium ion. Acta Crystallographica, B28, 683–693.

Liebau, F. (1972) Silicon. In D. M. Shaw, Ed., Handbook of Geochemistry, II/3, Sect. 14, Springer-Verlag, Berlin.

Liebau, F. (1980) Classification of silicates. Reviews in Mineralogy, 5, 1–24.

Lima-de-Faria, J. (1983) A proposal for a structural classification of minerals. Garcia de Orta, Séries Geologia, Lisboa, 6, 1–14.

Lima-de-Faria, J. and Figueiredo, M. O. (1976) Classification, notation and ordering on a table of inorganic structure types. Journal of Solid State Chemistry, 16, 7–20.

Loeb, A. L. (1970) A systematic survey of cubic crystal structures. Journal of Solid State Chemistry, 1, 237–267.

Makovicky, E. (1981) The building principles and classification of bismuth-lead sulphosalts and related compounds. Fortschritte der Mineralogie, 59, 137–190.

Mellini, M. (1981) Refinement of the crystal structure of låvenite. Tschermaks Mineralogische und Petrographische Mitteilungen, 28, 99–112.

Mellini, M. and Merlino, S. (1979) Refinement of the crystal structure of wohlerite. Tschermaks Mineralogische und Petrographische Mitteilungen, 26, 109–123.

Menchetti, S. and Sabelli, C. (1976) The halotrichite group: the crystal structure of apjohnite. Mineralogical Magazine, 40, 599–608.

Mereiter, K. (1974) Die Kristallstruktur von Rhomboklas, $H_5O_2^+\{Fe[SO_4]_2 \cdot 2H_2O\}^-$. Tschermaks Mineralogische und Petrographische Mitteilungen, 21, 216–232.

Moore, P. B. (1975) Brianite, $Na_2CaMg[PO_4]_2$: a phosphate analog of merwinite, $Ca_2CaMg[SiO_4]_2$. American Mineralogist, 60, 717–718.

Moore, P. B. (1980) The natural phosphate minerals: crystal chemistry. International Mondial du Phosphate. Second International Congress (Boston), 105–130.

Moore, P. B. and Araki, T. (1972) Atomic arrangement of merwinite, $Ca_2Mg[SiO_4]_2$, an unusual dense-packed structure of geophysical interest. American Mineralogist, 57, 1355–1374.

Moore, P. B. and Araki, T. (1974) Jahnsite,

$CaMn^{2+}Mg_2(H_2O)_8Fe_2^{3+}(OH)_2[PO_4]_4$: a novel stereoisomerism of ligands about octahedral corner-chains. American Mineralogist, 59, 964–973.

Moore, P. B. and Araki, T. (1977) Overite, segelerite, and jahnsite: a study in combinatorial polymorphism. American Mineralogist, 62, 692–702.

Moore, P. B. and Ito, J. (1978) I. Whiteite, a new species, and a proposed nomenclature for the jahnsite–whiteite complex series. Mineralogical Magazine, 42, 309–316.

Moore, P. B., Araki, T., Kampf, A. R. and Steele, I. M. (1976) Olmsteadite, $K_2Fe_2^{2+}[Fe_2^{2+}(Nb,Ta)_2^{5+}O_4(H_4O)_4(PO_4)_4]$, a new species, its crystal structure and relation to vauxite and montgomeryite. American Mineralogist, 61, 5–11.

Moore, P. B., Irving, A. J. and Kampf, A. R. (1975) Foggite, goedkenite and samuelsonite: three new species from the Palermo No. 1 pegmatite, North Groton, New Hampshire. American Mineralogist, 60, 957–964.

Nichols, M. C. (1966) The structure of tsumebite. American Mineralogist, 51, 267.

Nikitin, A. V. and Belov, N. V. (1962) Crystal structure of batisite $Na_2BaTi_2Si_4O_{14} = Na_2BaTi_2O_2[Si_4O_{12}]$. Doklady Akademii Nauk SSSR, 146, 142–143.

O'Keefe, M. and Hyde, B. G. (1980) Plane nets in crystal chemistry. Philosophical Transactions of the Royal Society of London, A. Mathematical and Physical Sciences, 295, 553–623.

Otto, H. H. (1975) Die Kristallstruktur von Fleischerit, $Pb_3Ge[(OH_6|(SO_4)_2] \cdot 3H_2O$, sowie kristallchemische Untersuchungen an isotypen Verbindungen. Neues Jahrbuch für Mineralogie Abhandlungen, 123, 160–190.

Pabst, A. (1950) A structural classification of fluoaluminates. American Mineralogist, 35, 149–165.

Parthé, E. (1981) Structural features of rare-earth-rich transition-metal alloys. In M. O'Keefe and A. Navrotsky, Eds., Structure and Bonding in Crystals, II, p. 259–296. Academic Press, New York.

Pauling, L. (1960) The Nature of the Chemical Bond (3rd edition). Cornell University Press, Ithaca, New York.

Perrault, G., Boucher, C., Vicat, J., Cannillo, E. and Rossi, G. (1973) Structure cristalline du nenadkevichite $(Na,K)_{2-x}(Nb,Ti)(O,OH)Si_2O_6 \cdot 2H_2O$. Acta Crystallographica, B29, 1432–1438.

Robinson, P. D. and Fang, J. H. (1969) Crystal structures and mineral chemistry of double-salt hydrates: I. Direct determination of the crystal structure of tamarugite. American Mineralogist, 54, 19–30.

Rumanova, I. M. and Malitskaya, G. I. (1960) Revision of the structure of astrakhanite by weighted phase projection methods. Soviet Physics Crystallography, 4, 481–495.

Scordari, F. (1980) Structural considerations of some natural and artificial iron hydrated sulphates. Mineralogical Magazine, 43, 669–673.

Scordari, F. (1981a) Crystal chemical implications on some alkali hydrated sulphates. Tschermaks Mineralogische und Petrographische Mitteilungen, 28, 207–222.

Scordari, F. (1981b) Sideronatrite: a mineral with a $\{Fe_2(SO_4)_4(OH)_2\}$ guildite type chain. Tschermaks Mineralogische und Petrographische Mitteilungen, 28, 315–319.

Shen, J. and Moore, P. B. (1982) Törnebohmite, $RE_2Al(OH)[SiO_4]_2$: crystal structure and genealogy of Re(III)Si(IV) $\rightleftharpoons$ Ca(II)P(V) isomorphisms. American Mineralogist, 67, 1021–1028.

Shibaeva, R. P., Simonov, V. I. and Belov, N. V. (1964) Crystal structure of the Ca,Na,Zr,Ti silicate Rosenbuschite, $Ca_{3.5}Na_{2.5}Zr(Ti,Mn,Nb)[Si_2O_7]_2F_2O(F,O)$. Soviet Physics Crystallography, 8, 406–413.

Srikanta, S., Sequeira, A. and Chidambaram, R. (1968) Neutron diffraction study of the space group and structure of manganese-leonite, $K_2Mn(SO_4)_2 \cdot 4H_2O$. Acta Crystallographica, B24, 1176–1182.

Sturman, B. D. and Dunn, P. J. (1980) Gaitite, $H_2Ca_2Zn(AsO_4)_2(OH)_2$, a new mineral from Tsumeb, Namibia (South West Africa). Canadian Mineralogist, 18, 197–200.

Süsse, P. (1968) Die Kristallstruktur des Botryogens. Acta Crystallographica, B24, 760–767.

Wan, C., Ghose, S. and Rossman, G. R. (1978) Guildite, a layer structure with a ferric hydroxy-sulphate chain and its optical absorption spectra. American Mineralogist, 63, 478–483.

Wardle, R. and Brindley, G. W. (1972) The crystal structures of pyrophyllite, 1Tc, and of its dehydroxylate. American Mineralogist, 57, 732–750.

Wood, M. M. (1970) The crystal structure of ransomite. American Mineralogist, 55, 729–734.

Ya-hsien, K., Simonov, V. I. and Belov, N. V. (1963) Crystal structure of bafertisite $BaFe_2TiO[Si_2O_7](OH)_2$. Doklady Akademii Nauk SSSR, 149, 123–126.

Zoltai, T. (1960) Classification of silicates and other minerals with tetrahedral structures. American Mineralogist, 45, 960–973.

Manuscript received, September 29, 1983.
accepted for publication, December 12, 1984.